ORIGINAL ARTICLE

Journal of Neurochemistry JNC The Official Journal of the International Society for Neurochemistry WILEY

Truncated GPNMB, a microglial transmembrane protein, serves as a scavenger receptor for oligomeric β-amyloid peptide$_{1\text{-}42}$ in primary type 1 microglia

Kohichi Kawahara[1,2] | Takuya Hasegawa[1] | Noa Hasegawa[1] | Taisei Izumi[1] | Koji Sato[3] | Toshiyuki Sakamaki[3] | Masayuki Ando[4] | Takehiko Maeda[1]

[1]Department of Pharmacology, Niigata University of Pharmacy and Medical and Life Sciences, Niigata, Japan

[2]Department of Bio-analytical Chemistry, Niigata University of Pharmacy and Medical and Life Sciences, Niigata, Japan

[3]Laboratory of Health Chemistry, Niigata University of Pharmacy and Medical and Life Sciences, Niigata, Japan

[4]Education Center for Pharmacy, Faculty of Pharmacy, Niigata University of Pharmacy and Medical and Life Sciences, Niigata, Japan

Correspondence
Kohichi Kawahara, Department of Bio-analytical Chemistry, Faculty of Pharmacy, Niigata University of Pharmacy and Medical and Life Sciences, 265-1 Higashijima, Akiha-ku, Niigata 956-8603, Japan.
Email: kkawa@nupals.ac.jp

Abstract

Glycoprotein non-metastatic melanoma protein B (GPNMB) is up-regulated in one subtype of microglia (MG) surrounding senile plaque depositions of amyloid-beta (Aβ) peptides. However, whether the microglial GPNMB can recognize the fibrous Aβ peptides as ligands remains unknown. In this study, we report that the truncated form of GPNMB, the antigen for 9F5, serves as a scavenger receptor for oligomeric Aβ$_{1\text{-}42}$ (o-Aβ$_{1\text{-}42}$) in rat primary type 1 MG. ^{125}I-labeled o-Aβ$_{1\text{-}42}$ exhibited specific and saturable endosomal/lysosomal degradation in primary-cultured type 1 MG from GPNMB-expressing wild-type mice, whereas the degradation activity was markedly reduced in cells from *Gpnmb*-knockout mice. The *Gpnmb*-siRNA significantly inhibits the degradation of ^{125}I-o-Aβ$_{1\text{-}42}$ by murine microglial MG5 cells. Therefore, GPNMB contributes to mouse MG's o-Aβ$_{1\text{-}42}$ clearance. In rat primary type 1 MG, the cell surface expression of truncated GPNMB was confirmed by a flow cytometric analysis using a previously established 9F5 antibody. ^{125}I-labeled o-Aβ$_{1\text{-}42}$ underwent endosomal/lysosomal degradation by rat primary type 1 MG in a dose-dependent fashion, while the 9F5 antibody inhibited the degradation. The binding of ^{125}I-o-Aβ$_{1\text{-}42}$ to the rat primary type 1 MG was inhibited by 42% by excess unlabeled o-Aβ$_{1\text{-}42}$, and by 52% by the 9F5 antibody. Interestingly, the ^{125}I-o-Aβ$_{1\text{-}42}$ degradations by MG-like cells from human-induced pluripotent stem cells was inhibited by the 9F5 antibody, suggesting that truncated GPNMB also serve as a scavenger receptor for o-Aβ$_{1\text{-}42}$ in human MG. Our study demonstrates that the truncated GPNMB (the antigen for 9F5) binds to oligomeric form of Aβ$_{1\text{-}42}$ and functions as a scavenger receptor on MG, and 9F5 antibody can act as a blocking antibody for the truncated GPNMB.

KEYWORDS
Alzheimer's disease, GPNMB/osteoactivin, oligomeric β-amyloid$_{1\text{-}42}$ (o-Aβ$_{1\text{-}42}$), scavenger receptor

1 | INTRODUCTION

Glycoprotein non-metastatic melanoma protein B (GPNMB) is a type I transmembrane glycoprotein that belongs to the same family as PMEL17 (Chrystal et al., 2021). PMEL17 is expressed only in melanin-producing cells, but GPNMB is widely expressed in dendritic cells, macrophages, osteoclasts, and microglia (MG) other than melanin-producing cells (Chrystal et al., 2021). PMEL17 acts as a scaffold protein for melanin synthesis and is involved in forming physiological amyloid (Hee et al., 2017; Theos et al., 2005). Because of its wide expression other than melanin-producing cells, GPNMB and PMEL17 are considered to have different functions, even though they belong to the same family of proteins. However, as PMEL17 and GPNMB share a common domain, such as the core amyloid fragment (CAF) domain (Chrystal et al., 2021), it is possible that some common evolutionarily conserved function exists.

Interestingly, Gpnmb was recently identified as one of the causative genes for cutaneous amyloidosis (Qin et al., 2021; Yang et al., 2018). That is, when the function of GPNMB decreased (loss of function of Gpnmb), amyloid was accumulated (Qin et al., 2021; Yang et al., 2018). In addition, the gene mutation was concentrated in the CAF domain (Chrystal et al., 2021). These results suggest that GPNMB is a molecule that controls the formation of "pathological" amyloid, as opposed to PMEL17 being involved in the formation of "physiological" amyloid.

In the central nervous system, GPNMB is expressed on one subtype of MG in the developing and the diseased brain (Kamphuis et al., 2016; Kawahara et al., 2016; Krasemann et al., 2017; Smith et al., 2022). GPNMB is expressed in the brain of patients with Alzheimer's disease (AD), and interestingly, it is expressed on MG around amyloid plaques (Hüttenrauch et al., 2018; Satoh et al., 2019; Smith et al., 2022). However, the function of GPNMB in amyloid metabolism has not been fully elucidated.

Recent studies have also revealed that GPNMB binds to "fibrous" carbon nanotubes and dermatophytes in mouse macrophage-like cell lines and mouse dendritic cells (Chung et al., 2009; He et al., 2018). However, whether microglial GPNMB binds directly to "fibrous" amyloid-beta (Aβ) is not yet clear. Most recently, Zhu et al. (2022) reported that the transduction of Gpnmb into the brain of mice serving as AD models reduced the Aβ accumulation in their hippocampi and improved their spatial memory impairment. The overexpression of Gpnmb increased the Aβ clearance activity of the microglial cell line BV2 (Zhu et al., 2022). However, the mechanism of Aβ clearance by GPNMB is not fully understood. According to the study by Zhu et al. (2022), autophagy is involved in Aβ clearance induced by GPNMB. However, it is unclear how GPNMB is involved in the upstream mechanism of autophagy. It is also unknown whether the endogenous GPNMB is a molecule that contributes to the Aβ clearance undertaken by MG.

It is conceived that there may be at least two subtypes of MG in CNS, and each subtype may play a particular role (Hanisch, 2013; Prinz et al., 2021). For example, we have reported that anti-inflammatory cytokine interleukin-4 enhances clearance of oligomeric Aβ$_{1-42}$ by

rat type 2 MG (Shimizu et al., 2008), whereas lipopolysaccharide induced the expression of inflammatory molecules (iNOS and TNF-α) more markedly in type 1 MG than those in type 2 (Kawahara et al., 2009).

To differentiate subtypes of MG, we recently developed a novel monoclonal antibody, 9F5, against rat type 1 MG, and the antigen was GPNMB (Kawahara et al., 2016). The 9F5 antibody does not react with full-length GPNMB and specifically recognizes the truncated GPNMB cleaved by the furin-like protease at the site of K^{169}-K^{170} (Kawahara et al., 2016). The antigen for 9F5 (truncated GPNMB) is expressed in one subtype of MG in the developing rat brain (Kawahara et al., 2016). However, the function of the truncated GPNMB in MG is completely unknown.

In the present study, we investigated whether the GPNMB expressed in MG can directly interact with the oligomeric form of Aβ$_{1-42}$ (o-Aβ$_{1-42}$), a most neurotoxic species of Aβ (Haass & Selkoe, 2007; Laurén et al., 2009; van Dyck et al., 2023). Most experiments were evaluated by cellular assays, as amyloid is highly hydrophobic and exerts non-specific binding. Herein, we provide evidence, suggesting that the antigen for 9F5 (truncated GPNMB), expressed on the cell surface of primary-cultured type 1 MG, functions as a scavenger receptor for oligomeric Aβ$_{1-42}$ and the 9F5 monoclonal antibody can act as a blocking antibody for the truncated GPNMB on rat and human MG.

2 | MATERIALS AND METHODS

2.1 | Chemicals and materials

Anti-CD40 antibody (Santa Cruz Biotechnology, RRID:AB_2244535), anti-iNOS antibody (BD Transduction Laboratories, RRID:AB_2890165), and anti-β-actin antibody (Sigma-Aldrich, RRID:AB_476744) were used. Purified mouse monoclonal anti-rat truncated GPNMB/osteoactivin antibody (9F5; IgG$_1$) was prepared as previously described (Kawahara et al., 2016). Mouse monoclonal anti-human SRA antibody (SRA-E5) was a gift from Prof. M. Takeya (Kumamoto University, Kumamoto, Japan). Recombinant mouse GPNMB-Fc (2330-AC) and human GPNMB-Fc (2550-AC) were purchased from R&D Systems. Other chemicals were of the highest grade available from commercial sources.

2.2 | Protein purification

Size exclusion chromatography (SEC) was performed as previously described (Walsh et al., 1997). Sephadex G-100 media (superfine, Sigma-Aldrich) were prepared by using either a 1×30 cm or a 1×50 cm Econo column (Bio-Rad, CA), were eluted at 0.11 mL/min by using a peristaltic pump (Micro tube pump MP-3, EYELA, Japan), and were then fractionated by a fraction collector (CHF100A, ADVANTEC, Japan). For each study, the column was equilibrated with at least three column volumes of elution buffer (PBS) and

then calibrated with six molecular weight standards: blue dextran (2 000 000); bovine serum albumin (66 000); bovine carbonic anhydrase (29 000); horse cytochrome c (12 400); bovine aprotinin (6500); and N-(2,4-dinitrophenyl)-L-alanine (255). Sephadex G-100 columns were prepared from fresh resin prior to each experiment.

2.3 | Preparation of o-Aβ$_{1-42}$

o-Aβ was prepared as previously described (Shimizu et al., 2008) and slightly modified. The chloride form of the Aβ$_{1-42}$ peptides (AnaSpec Inc., CA) was initially dissolved in hexafluoroisopropanol (Sigma-Aldrich) to achieve a concentration of 1 mM. The solution was then separated into aliquots in sterile microcentrifuge tubes. Hexafluoroisopropanol was removed under vacuum in a SpeedVac concentrator, and the peptide film was stored in a desiccated form at −25°C. The peptide was first resuspended in dry dimethyl sulfoxide to a concentration of 5 mM for the aggregation protocol on a preparative scale. Ham's F-12 (Invitrogen) was then added to bring the peptide to a final concentration of 500 μM, and the samples were rotated on a rotary shaker at 4°C for 24 h. o-Aβ$_{1-42}$ prepared as above (271–452 μg in PBS) was radioiodinated by the Iodo-Gen method with Na^{125}I (PerkinElmer) at 7.4–18.5 MBq. Excess ^{125}I was removed by a Sephadex G-100 column or equilibrated with PBS using Spectra/Por 7 (MWCO 1000). The specific activity of the ^{125}I-labeled Aβ$_{1-42}$ was 183–427 cpm/ng.

2.4 | Silver stain, autoradiography, and immunoblot analysis

SDS-PAGE was carried out on 10%–20% gels (EHR-T1020L, ATTO Co., Japan). Aliquots of each chromatographic fraction (8 μL) were mixed with 5× SDS sample buffer (2 μL) under non-reducing conditions and were incubated at 60°C for 10 min immediately prior to electrophoresis. Gels were silver-stained by using a silver stain kit (291–50 301, Wako, Japan) and were subsequently photographed. For autoradiography, the gels were dried and contacted with X-ray film (RX-U, Fujifilm, Japan). After 48–96 h, the films were developed and fixed by using Korectol E (Fujifilm) and Super Fujifix-L (Fujifilm), respectively. For the western blotting analysis, the samples were subjected to SDS-PAGE and electrotransferred to a PVDF membrane. The membrane was incubated with an antibody against Aβ$_{1-16}$ (6E10; 1:500 dilution, BioLegend, RRID:AB_2728533), followed by horseradish peroxidase (HRP)-linked antibody against mouse immunoglobulins (1:1000 dilution). Bound HRP-labeled antibodies were then detected via chemiluminescence (ECL kit).

2.5 | Animals

Wistar rats and C57BL/6J mice were obtained from The Jackson Laboratory Japan, Inc. Gpnmb-knockout mice [Gpnmb$^{tm1(Gfp)Mcf}$]

were generated as previously described (Kawahara et al., 2016). Hemizygous APP23 mice, which overexpress human-type Aβ precursor protein (APP) carrying the double-mutation K670 N/M671 L, were produced and bred as previously described (Kawahara et al., 2014; Sturchler-Pierrat et al., 1997). Hemizygous male APP23 mice were crossing with heterozygous female Gpnmb$^{+/-}$ mice to get APP23;Gpnmb$^{+/-}$ mice. Subsequently, male APP23;Gpnmb$^{+/-}$ mice were crossed with female Gpnmb$^{+/-}$ or Gpnmb$^{-/-}$ mice to get APP23;Gpnmb$^{-/-}$ mice. Hemizygous 5xFAD (RRID:MMRRC_0340-JAX; Oakley et al., 2006) were obtained from Jackson Laboratory. Hemizygous male 5xFAD mice were backcrossed to C57BL/6J for at least 10 generations before crossing with heterozygous female Gpnmb$^{+/-}$ or Gpnmb$^{-/-}$ mice to get 5xFAD;Gpnmb$^{-/-}$ mice. Male and female mice were analyzed. The mice for immunohistochemistry and monitoring survival were housed (one to five mice in each rectangular plastic cage) in a pathogen-free facility under 12/12 h light/dark conditions with ad libitum access to pelleted mouse food and water. Totally, 753 mice were used for immunohistochemistry and survival monitoring experiments. The animal experiments were conducted according to the guidelines of the Ministry of Education, Culture, Sports, Science, and Technology of Japan, and were approved by the Institutional Animal Care and Use Committee of the Niigata University of Pharmacy and Medical and Life Sciences (#18–2, #19–6, #19–29, #21–3, #21–4, #22–3, #22–22, and #23–3).

2.6 | Cell culture

Rat and mouse primary MG were harvested from primary mixed glial cell cultures (mixed sex) prepared from neonatal Wistar rats, Gpnmb$^{+/+}$ (WT) mice, and Gpnmb$^{-/-}$ (KO) mice as previously reported (Kawahara et al., 2016; Sawada et al., 1990; Shimizu et al., 2008; Suzumura et al., 1987). The pups were killed by decapitation. A total of 442 animals (including dams and pups) were used for cell culture experiments. Brains were pooled before plating. In brief, after the meninges were carefully removed, the neonatal brain (at post-natal day 0–2) was dissociated by pipetting. The cell suspension was added to 75-cm^2 culture flasks at a density of one brain per two flasks (for rats) or two brains per flask (for mice), in 10 mL of Eagle's MEM supplemented with 10% fetal bovine serum (FBS), 5 μg/mL human insulin, and 0.2% glucose. Type 1 MG was isolated on days 14–16 by the "shaking off" method as previously described (Sawada et al., 1990). Type 2 MG (see Figure 2) were isolated on days 16–19 by harvesting with 5 mM EDTA in phosphate buffer solution as reported previously (Shimizu et al., 2008). Murine microglial MG5 cells were maintained as described (Kawahara et al., 2001; Ohsawa et al., 1997). Human MG-like cells (Cellartis Microglia) from human iPSCs (ChiPSC12, male, age 24) were maintained according to the manufacturer's recommendations (Takara-Bio Inc., Japan). The five vials of the Cellartis Microglia (Lot #AK30017S) and five bottles of culture medium (Lot#AK4L025, three bottles and #AL50012S, two bottles) were used in the present study (from November 2020 to March 2022).

The Cellartis Microglia have functions such as phagocytosis of amyloid-β, ATP-responsive migration, and cytokine release in response to lipopolysaccharide (Takara-Bio Inc.).

2.7 | Immunocytochemical analysis

Rat and mouse primary type 1 MG were plated on 8-well Lab-Tek chamber slides (Nalge Nunc International) and were cultured for 1 day. MG-like cells from human iPSCs were plated on 8-well BioCoat poly-D-lysine/laminin culture slides (Corning) and were cultured for 4 days. For some experiments, rat type 1 MG was cultured for 2 h in MEM containing 10% FBS, in the presence or absence of o-Aβ_{1-42} (1 or 2 μg/mL; see Figures 5b and 7). The cells were then incubated with 9F5 (1 μg/mL; mouse IgG$_1$), rabbit anti-Iba1 (2.5 μg/mL; Wako, RRID:AB_839504), goat anti-mouse GPNMB (AF2330, 1 μg/mL; R&D, RRID:AB_2112934), rabbit anti-Aβ antibody (D54D2, 1:500; Cell Signaling Technology), or the isotype-matched controls. Alexa Fluor 488- or 594-labeled secondary antibodies (1:400; Invitrogen) were used. Nuclei were stained by Hoechst 33258 (0.008% w/v; Sigma). Stained cells were observed with a confocal laser scanning microscope (LSM700, Carl Zeiss; Fluoview FV-1000, Olympus).

2.8 | Immunofluorescent flow cytometry

Rat type 1 MG (1×10^6 cells in 200 μL) were incubated with mouse monoclonal antibody against rat truncated GPNMB (10 μg/mL; 9F5), mouse IgG$_1$ (10 μg/mL; 15H6, Southern Biotechnology Associates Inc.), goat polyclonal antibody against mouse GPNMB (10 μg/mL; AF2330), and normal goat IgG (10 μg/mL; AB-108-C, R&D Systems), at 4°C for 30 min, followed by an incubation with an Alexa Fluor 488-labeled secondary antibody (1:400; Invitrogen), and were analyzed using a fluorescence-activated cell sorter (CytoFLEX, Beckman Coulter).

2.9 | siRNA transfection

Small interfering RNAs (siRNAs) for targeting of mouse *Gpnmb*/DC-HIL (DC-HIL siRNA no. 3, sense 5′-r(AACUUGUCUGAUGAGAUCU)dTdT-3 and antisense 5′-r(AGAUCUCAUCAGACAAGUU)dTdT-3; DC-HIL siRNA no. 10, sense 5′-r(GCGUACAAGCCAAUAGGAA)dTdT-3 and antisense, 5′-r(UUCCUAUUGGCUUGUACGC)dTdT-3; Chung et al., 2007) were obtained from Sigma-Aldrich. MG5 cells (2×10^6 cells) were transfected with a mixture of DC-HIL siRNAs no. 3 and no. 10 (each 1.5 μg) by using Nucleofector 2b (AAB-1001, Lonza). As a negative control, MISSION® siRNA universal negative control #1 (3 μg; Sigma-Aldrich) was transfected. After a 72-h incubation, these transfected MG5 cells were harvested and examined by western blotting for the protein expression of DC-HIL/GPNMB by using a goat anti-mouse GPNMB antibody (0.4 μg/mL; AF2330).

2.10 | Cell-based assays for Aβ metabolism

Mouse and rat type 1 MG (1.5×10^5 cells in 48-well, 2×10^5 cells in 24-well) and mouse type 2 MG (2×10^5 cells in 24-well; see Figure 2) were cultured in 48-well or 24-well plates, for 24 h, in MEM containing 10% FBS. Mouse MG5 cells (1.25×10^5 cells) transfected with Gpnmb/DC-HIL siRNA or control siRNA were cultured in 24-well plates, for 72 h, in DMEM containing 10% FBS. Human iPSCs-derived MG-like cells (6×10^4 cells) were cultured in poly-D-lysine/laminin cellware 96-well plates (Corning), for 96 h, in culture medium for Cellartis MG (Y50042, Takara-Bio) before start of the experiment. Cells were washed twice with a labeling medium (DMEM containing 3% bovine serum albumin; BSA) and were then incubated with ^{125}I-labeled o-Aβ_{1-42} for 6 h, at 37°C, in a 5% CO$_2$-humidified air atmosphere. Following the 6-h incubation, medium was removed from each well, and the soluble radioactivity in trichloroacetic–acid–silver–nitrate (degraded and extracellularly released peptide fragments) was determined as an index of the Aβ degradation in the medium as previously described (Hakamata et al., 1995; Kawahara et al., 2014; Shimizu et al., 2008). The microglia protein in the wells was determined after dissolving the cells in 0.1 M NaOH (0.4 mL), for 30 min at 37°C. Data are expressed as micrograms of o-Aβ_{1-42} degraded during the 6 h per mg of microglia protein. The Aβ degradation activity may, thus, include both receptor-mediated phagocytic activity and extracellular protease-mediated degradation. Cells were washed three times with PBS and were then lysed with 0.4 mL (for 24-well) or 0.2 mL (for 48-well) of 0.1 M NaOH, for 30 min at 37°C. At the same time, cell-associated (including the cell-incorporated) radioactivity and cell proteins were determined with an automatic γ-counter and the BCA Protein Assay Reagent (Pierce), respectively. In the case of 96-well plates, cells were lysed with 70 μL of 0.1 M NaOH for 30 min at 37°C, and 15 μL of 1 M Tris–HCl (pH 7.4) were added to each well; subsequently, the cell-associated (including the cell-incorporated) radioactivity and cell proteins were determined with an automatic γ-counter and Bradford Assay Reagent (Pierce), respectively.

Since exact molecular weight of SEC-isolated o-Aβ_{1-42} is unknown (Figure 1a), o-Aβ could not be expressed as the amount of substance (*n*, mol). In the present study, the molar concentration of o-Aβ_{1-42} was described as a monomer equivalent of total Aβ_{1-42} (Kim et al., 2013; Laurén et al., 2009), and the molecular weight of Aβ_{1-42} was calculated as 4514.

2.11 | Enzyme-linked immunosorbent assay (ELISA)

The TBS-soluble (TBS-extractable) fraction and the TBS-insoluble (but guanidine HCl-extractable) fraction from hippocampus were prepared as described previously (Kawahara et al., 2014). The amounts of Aβ_{42} in each fraction were determined by using sandwich ELISA (#290–62601, Wako), according to the manufacturer's instructions. Protein concentrations were determined with the BCA Protein Assay Reagent (Pierce), with BSA as the standard.
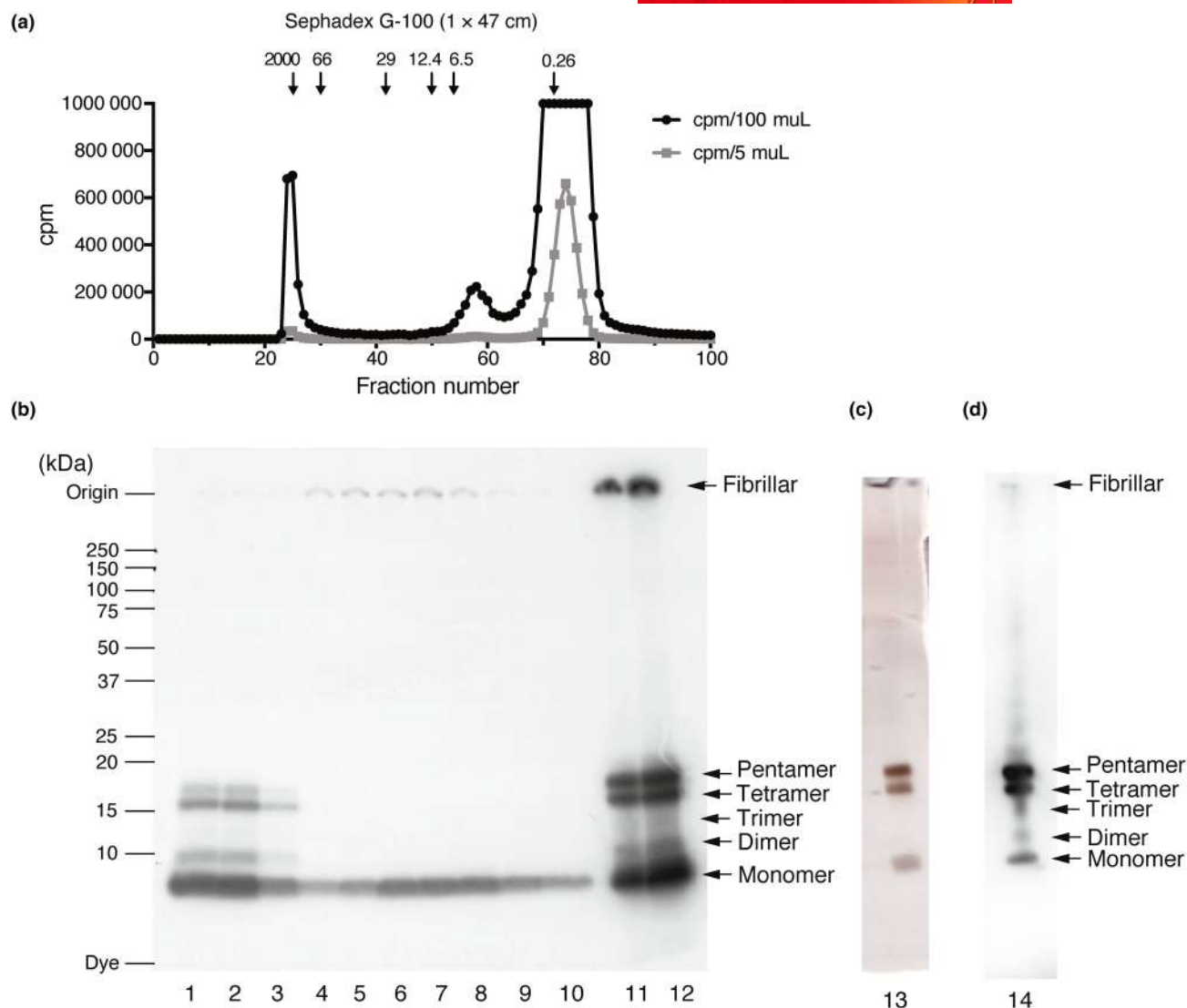
FIGURE 1 Characterization of the ^{125}I-labeled o-A$\beta_{1\text{-}42}$. (a) SEC of o-A$\beta_{1\text{-}42}$. ^{125}I-labeled o-A$\beta_{1\text{-}42}$ (254 μg) was chromatographed on a Sephadex G-100 column (1.0 × 47 cm), and was fractionated per 0.5 mL each. The radioactivity of 5-μL or 100-μL aliquots from each fraction was determined by using a γ-counter. The gel-included peak elutes at ca. 29 mL (fraction number 58) and at ca. 37 mL (fraction number 74), while the gel-excluded peak elutes at ca. 12.5 mL (fraction number 25). Arrows indicate elution positions of the molecular weight standards. Molecular masses are indicated in kDa. (b) Autoradiography of SEC fractions. ^{125}I-labeled o-A$\beta_{1\text{-}42}$ was fractionated by SEC (as described under Figure 1a) and was then analyzed by SDS-PAGE and autoradiography. Samples derived from 8-μL aliquots of the gel-excluded peak fractions (lanes 1–3: fraction numbers 24–26, respectively) and of the fractions of the monomer peaks (lanes 4–10: fraction numbers 55–61, respectively). Lanes 11 and 12 represent the aliquots (1.0 and 2.6 μg, respectively) of the pre-chromatography samples. Additional results are shown in Figures S1 and S2. (c, d) Silver stain (c) and western blotting analysis using 6E10 (anti-A$\beta_{1\text{-}16}$ antibodies) (d) of pre-chromatography samples (1.0 μg in C and 0.4 μg in d) of o-A$\beta_{1\text{-}42}$.

2.12 | Immunoprecipitation

Antibodies were bound to Protein G-Sepharose 4 Fast Flow gel (GE Healthcare) by incubating a mixture of anti-Aβ antibodies (5 μg of 6E10 antibody and 2 μg of D54D2 antibody; in 110 μL of TBS), 15 μL of ascites fluid of 9F5 antibody (diluted 1:10 in TBS), or 80 μg of mouse IgG$_1$ (in 180 μL of TBS) with 50 μL of the swollen gel in buffer A [10 mM Tris–HCl (pH 7.4), 150 mM NaCl, 0.1% NP-40, and protease inhibitors] at 4°C overnight. The gel was washed 2 times with buffer A (at 2250 g for 20 s at 4°C) before adding lysates of

rat type 1 MG (ca. 132 μg per tube, ca. 5 × 10^6 cells per tube) for overnight incubation at 4°C. After the sample was washed 1 time with buffer B [10 mM Tris–HCl (pH 7.4), 150 mM NaCl, 1% NP-40, and protease inhibitors] and 2 times with buffer A, immunoprecipitated proteins were extracted from the gel with 90 μL of sampling buffer for SDS-PAGE [50 mM Tris–HCl (pH 6.8), 4% (w/v) SDS, and 12% (v/v) glycerol] for 10 min at 70°C and an aliquot (10 μL) was separated by SDS-PAGE and transferred to PVDF membranes. The PVDF membranes were immunoblotted to antibodies against GPNMB and Aβ.

1322 | WILEY- Journal of Neurochemistry **JNC** *The Official Journal of the International Society for Neurochemistry*

KAWAHARA ET AL.

2.13 | Detection of protein–protein interaction using in situ proximity ligation assay

The interactions between Aβ peptides and rat GPNMB were assayed using Duolink in situ detection reagents red (#DUO92008, Sigma-Aldrich), as instructed by a manufacturer. Briefly, rat type 1 MG were plated on 8-well BioCoat poly-D-lysine/laminin culture slides (Corning) and were cultured for 1 day. Rat type 1 MG were incubated for 30 min in MEM containing 10% FBS in the presence or absence of 100 µg/mL of fucoidan and were then cultured for 2 h in MEM containing 10% FBS in the presence or absence of o-Aβ_{1-42} (2 µg/mL). After incubation, the cells were fixed in 4% paraformaldehyde phosphate buffer solution for 10 min at room temperature. After washing with PBS, the cells were incubated with 0.05% Triton X-100 in PBS for 10 min to permeabilize cell membranes. The cells were then blocked with 2.5% BSA in PBS for 30 min at 4°C. The cells were then incubated with 9F5 (1 µg/mL), goat anti-mouse GPNMB (AF2330, 1 µg/mL), or rabbit anti-Aβ antibody (D54D2, 1:500) for overnight at 4°C. The cells were washed with PBS and Wash buffer A (10 mM Tris–HCl (pH 7.4), 150 mM NaCl, 0.05% Tween-20) and incubated in PLA probe plus and minus solution (#DUO92002, #DUO92004, #DUO92006, Sigma-Aldrich) for 1 h at 37°C, in a 5% CO_2-humidified air atmosphere. The cells were washed 2 times with Wash buffer A and incubated with Ligation-Ligase solution (#DUO92008) for 30 min at 37°C, in a 5% CO_2-humidified air atmosphere. The cells were washed 2 times with Wash buffer A and incubated with Amplification Red-Polymerase solution (#DUO92008) for 90 min at 37°C, in a 5% CO_2-humidified air atmosphere. The cells were washed 1 time with Wash buffer B [200 mM Tris–HCl (pH 7.5) and 100 mM NaCl], 1 time with Wash buffer B containing Hoechst 33258 (80 µg/mL), and 1 time with Wash buffer C [0.1 mM Tris–HCl (pH 7.4), 1.5 mM NaCl, 0.0005% Tween-20]. The cells were mounted with VECTASHIELD PLUS Antifade Mounting Medium (Vector). Stained cells were observed with a confocal laser scanning microscope (Fluoview FV-1000, Olympus). Fluorescence intensity was quantified via the NIH ImageJ software obtained from a public web site (http://rsb.info.nih.gov/nih-image/).

2.14 | Immunohistochemistry

The paraffin tissue sections "Alzheimer's Disease: Brain: Hippocampus" (from an 88-year-old man; #T2236052ALZ) were purchased from BCH BioChain Institute Inc. (Newark, CA). These tissue sections were incubated at 60°C for 1 h for baking. After deparaffination, the tissue sections were incubated with proteinase K (10 µg/mL) at 37°C for 10 min. They were then treated at room temperature for 30 min with 0.3% hydrogen peroxide–containing methanol to block endogenous peroxidase activity. Subsequently, the sections were incubated with G-Block reagent (GB-01, Genostaff) at room temperature for 10 min. To block endogenous biotin activity, a biotin blocking system (Vector) was used. The tissue sections were then

incubated with 9F5 antibody (2 µg/mL, diluted with 1% G-Block/TBS) at 4°C for 18 h. After washing with TBS-T and TBS three times, the tissue sections were incubated with biotin-conjugated anti-mouse secondary antibody (Nichirei, Japan) at room temperature for 30 min, followed by horseradish peroxidase–conjugated streptavidin (Nichirei) at room temperature for 5 min. After washing, the tissue sections were incubated with diaminobenzidine tetrahydrochloride substrate. Subsequently, they were processed for counterstaining with hematoxylin. As a negative control, normal mouse IgG_1 (X0931, Dako) was used. Some sections were stained with 0.01% (w/v) 1-fluoro-2,5-bis(3-carboxy-4-hydroxystyryl)benzene (FSB; a reagent used for amyloid staining; Dojindo, Japan) as described previously (Kawahara et al., 2014).

To minimize animal suffering during the experiment, mice were euthanized by intraperitoneal injection of an overdose of pentobarbital (100 mg/kg) before removal of the brain. Frozen sections (30-µm-thick) of the brain were incubated with 0.01% (w/v) FSB for 30 min. After washing with 50% ethanol, the sections were autoclaved (at 120°C) in 10 mM citrate buffer (pH = 6.0) for 5 min and washed in PBS. The sections were then incubated with primary antibodies to GPNMB (goat IgG, AF2330, 1 µg/mL) and Iba1 (rabbit IgG, 1:200 dilution), followed by the corresponding Alexa Fluor 488- or 594-labeled secondary antibodies (1:300 dilution; Invitrogen).

2.15 | AlphaFold2 prediction models

Protein structure prediction of the rat GPNMB was obtained from AlphaFold Protein Structure Database, which DeepMind developed (UK) and EMBL-EBI (UK), updated in AlphaFold DB version at June 1, 2022) and created with the AlphaFold Monomer v2.0. Pipeline. The visualization was made possible by using the 3D viewer of the database or by using the UCSF ChimeraX version 1.4 developed by the UCSF Resource for Biocomputing, Visualization, and Informatics.

The predicted alignment error (PAE) matrices, the coverage of multiple sequence alignment (MSA), and the predicted local difference distance test (lDDT) per residue of the rat GPNMB were constructed via ColabFold (Mirdita et al., 2022).

2.16 | Statistical analysis

Data were expressed as mean ± standard deviation (SD) or as mean ± range, as indicated in the Figure legends. No test for outliers was conducted in this study. For comparisons of three or more treatments, we applied Tukey's multiple comparison test after a one-way analysis of variance. Tests were two-tailed. No statistical method was used to determine the sample size. All statistical analyses were performed with GraphPad Prism7 (GraphPad Software). *p* values lower than 0.05 were considered statistically significant. Results of all statistical comparisons between experimental groups are shown in the separate Tables S1 and S2.

3 | RESULTS

3.1 | Characterization of ^{125}I-labeled o-A$\beta_{1\text{-}42}$

We prepared o-A$\beta_{1\text{-}42}$ according to a method described previously (Dahlgren et al., 2002; Shimizu et al., 2008), and a portion of the oligomer preparation was further iodinated with Na^{125}I via Iodo-Gen. Size exclusion chromatography (SEC) was also performed to remove the unpolymerized monomer A$\beta_{1\text{-}42}$. The prepared ^{125}I-labeled o-Aβ was separated by a Sephadex G-100 column (1.0×47 cm), its radioisotope (RI) count was measured, and three peaks were detected (Figure 1a). Of these, the third eluted peak had a molecular weight of about 0.26 kDa, thereby indicating that it corresponded to unbound ^{125}I. The first peak eluted near 2000 kDa, while the second peak eluted around 6.5 kDa; both were further analyzed by autoradiography. When the autoradiographic analysis was performed on the first peak fraction, four bands (monomers, dimers, tetramers, and pentamers) were detected (Figure 1b, lanes 1–3). In addition, when the autoradiographic analysis was performed on the second peak fraction, only one band (monomer) was detected (Figure 1b, lanes 4–10). These results indicate that the high molecular weight oligomer Aβ, eluted at around 2000 kDa by SEC, is dissociated into monomers, dimers, tetramers, and pentamers by SDS-PAGE. It is also suggested that the low molecular weight oligomer Aβ that was eluted near 6.5 kDa by SEC is a monomer.

When autoradiography was performed on the sample prior to the column separation (pre-chromatography sample), a fibrillar form was detected in addition to the monomers, dimers, tetramers, and pentamers (Figure 1b, lanes 11 and 12). Since fibrillar Aβ was not eluted from the column (Figure 1b, lanes 1–10), it is considered that Sephadex G-100 adsorbed it. The prepared ^{125}I-labeled o-A$\beta_{1\text{-}42}$ exhibited an electrophoretic pattern on SDS-PAGE that was similar to that of the unlabeled o-A$\beta_{1\text{-}42}$ (Figure 1b, lanes 11 and 12 vs. Figure 1c,d), as described previously (Shimizu et al., 2008).

We observed that the faint band of fibrillar Aβ was detected in lanes 1–3 as well as lanes 4–8 in enhanced image of the autoradiography (Figures S1 and S2). These results suggest that low amount of fibrillar Aβ is contained in the sample of SEC-isolated ^{125}I-o-A$\beta_{1\text{-}42}$ and ^{125}I-monomer-A$\beta_{1\text{-}42}$. Since A$\beta_{1\text{-}42}$ tends to aggregate, fibrillar A$\beta_{1\text{-}42}$ may have been generated after fractionation.

3.2 | Comparison of o-Aβ clearance by mouse primary type 1 and type 2 MG

We previously reported that interleukin-4 enhances the uptake of o-A$\beta_{1\text{-}42}$ by rat primary type 2 MG but not type 1 MG, although no difference was observed between the two subtypes under "unstimulated conditions" (Shimizu et al., 2008). We also previously identified truncated GPNMB as a selective marker for type 1 MG (Kawahara et al., 2016). However, both type 1 and type 2 MG expressed mRNA and the full-length GPNMB protein (Kawahara

et al., 2016). Therefore, in cellular assays, we initially compared the clearance activity of ^{125}I-o-A$\beta_{1\text{-}42}$ (>1 kDa) in mouse MG subtypes using the same method we previously used to compare that in rat MG subtypes.

We separated type 1 and type 2 MG from a mouse mixed glial cell culture using a method described previously (Shimizu et al., 2008). We confirmed that the lipopolysaccharide (LPS)-induced expression levels of CD40 and inducible nitric oxide synthase (iNOS) were higher in type 1 MG than in type 2 MG (Figure 2a,b), as previously reported (Kanzawa et al., 2000; Kawahara et al., 2009, 2016; Shimizu et al., 2008). The expression level of scavenger receptor type A (SRA) was similar in both MG types (Figure 2b), as previously reported (Shimizu et al., 2008). Figure 2c,d shows the expression level of GPNMB in both MG types according to immunoblot analysis with a polyclonal anti-GPNMB antibody (AF2330). Both MG types exhibited similar levels of full-length GPNMB (ca. 118.7 kDa), as previously reported (Kawahara et al., 2016). However, the expression levels of lower molecular weight GPNMB proteins (ca. 92.3, ca. 75.3, and 50–70 kDa) were higher in mouse type 1 MG than in type 2 MG (Figure 2c,d). We observed that LPS treatment exhibited mobility shift of SRA in gel (Figure 2b). However, we did not investigate the mechanism further, because we focused on the degradation activity of unstimulated cells in the present study.

Using these MG preparations, we found that the clearance of ^{125}I-o-A$\beta_{1\text{-}42}$ (>1 kDa) by type 1 MG was 1.5-fold higher than by type 2 MG (Figure 2e, column 1 vs. column 7). Scavenger receptors and cathepsin B contribute to the microglial o-Aβ clearance (Frenkel et al., 2013; Shibuya et al., 2014; Shimizu et al., 2008). The degradation activity in both MG types was suppressed by the addition of fucoidan, an inhibitor of various scavenger receptors (Figure 2e, columns 2 and 8), and CA074Me, a membrane-permeable inhibitor of cathepsin B (Figure 2e, columns 3 and 9), indicating that the scavenger receptors and intracellular cathepsin B contribute to the degradation of o-A$\beta_{1\text{-}42}$ in both MG types. We also found that the contribution of GPNMB to o-A$\beta_{1\text{-}42}$ clearance is selective in type 1 MG because the activity of type 2 MG from *Gpnmb*-deficient mice was indistinguishable from that of wild-type type 2 MG (Figure 2e, columns 1 and 4 vs. columns 7 and 10). We observed the contribution of GPNMB to fucoidan-sensitive and CA074Me-sensitive degradation activities of o-A$\beta_{1\text{-}42}$ in mouse primary type 1 MG, but not in type 2 MG (Figure S3).

3.3 | GPNMB contributes to o-Aβ clearance by mouse primary type 1 MG

Because we initially observed that GPNMB-mediated o-A$\beta_{1\text{-}42}$ clearance was dominant in type 1 MG but not type 2 MG (Figure 2e), we focused on type 1 MG in the present study, investigating the mechanism of this type in more detail. As ^{125}I-o-A$\beta_{1\text{-}42}$ (>1 kDa, used in the experiment shown in Figure 2) contained fibrillar and monomer forms (Figure 1; Figure S2), we isolated the high molecular
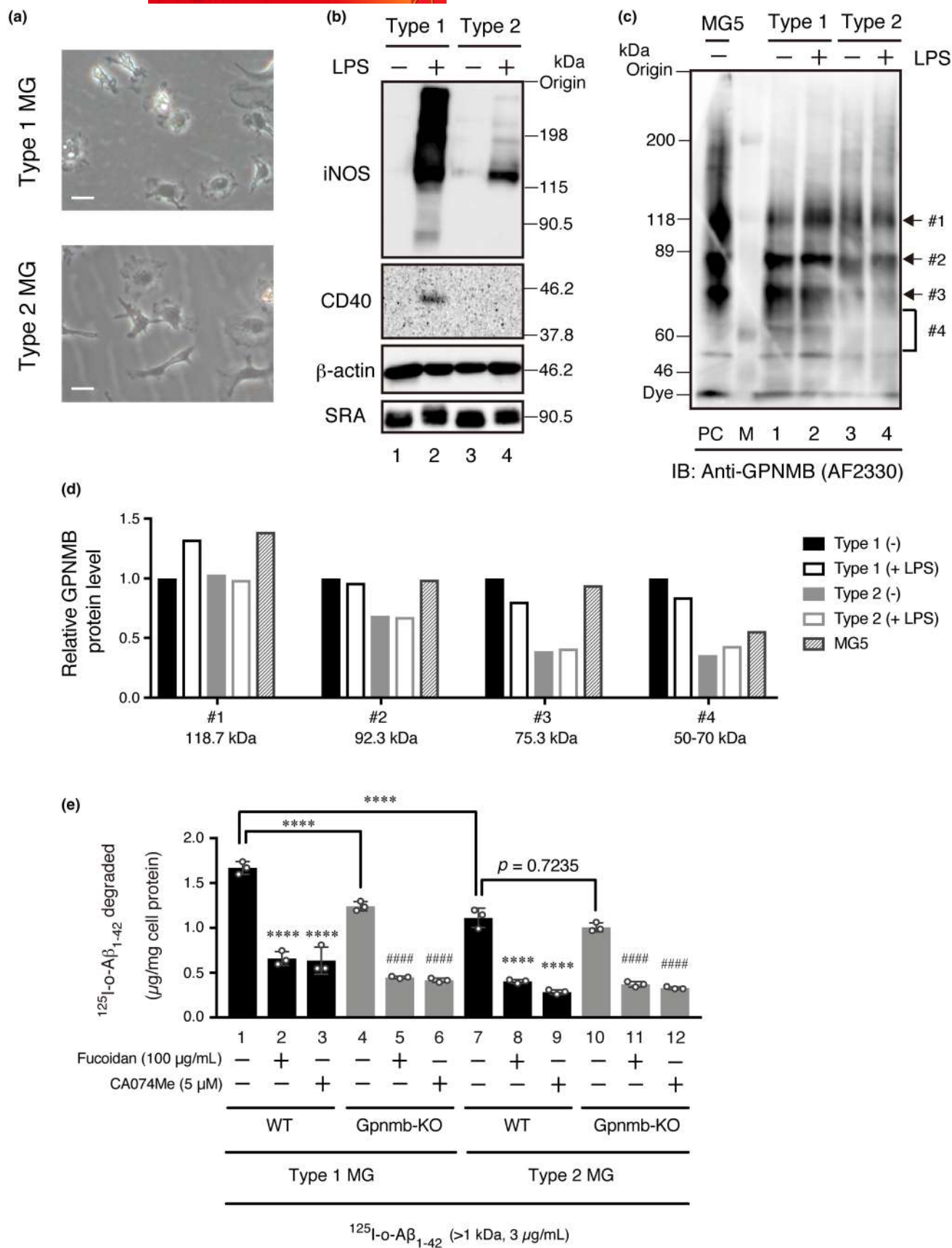
(a) Type 1 MG, Type 2 MG

(b) iNOS, CD40, β-actin, SRA — Type 1, Type 2, LPS

(c) IB: Anti-GPNMB (AF2330)

(d) Relative GPNMB protein level — #1 118.7 kDa, #2 92.3 kDa, #3 75.3 kDa, #4 50-70 kDa
Type 1 (−), Type 1 (+ LPS), Type 2 (−), Type 2 (+ LPS), MG5

(e) ^{125}I-o-Aβ_{1-42} degraded (μg/mg cell protein)
Fucoidan (100 μg/mL), CA074Me (5 μM)
WT, Gpnmb-KO, Type 1 MG, Type 2 MG
^{125}I-o-Aβ_{1-42} (>1 kDa, 3 μg/mL)

FIGURE 2 Degradation of ^{125}I-labeled o-Aβ_{1-42} by type 1 MG and type 2 MG in the mouse primary culture. (a–d) Mouse primary type 1 and type 2 MG were isolated as described in the *Materials and Methods*. (a) Phase-contrast images of the cells are shown. Bar: 20 μm. (b) Cells were (+) or were not (−) treated with lipopolysaccharide (LPS; 1 μg/mL) for 24 h. Protein concentrations of each cell lysates were determined with the BCA Protein Assay Reagent (Pierce), with BSA as the standard. Cell proteins (30 μg) were subjected to immunoblot analysis with antibodies against iNOS, CD40, β-actin, or scavenger receptor type A (SRA). (c) Cells were (+) or were not (−) treated with LPS (1 μg/mL) for 24 h. Cell proteins (30 μg) were subjected to immunoblot analysis with an antibody against GPNMB. Extracts (30 μg of protein) from mouse microglial MG5 cells were used as a positive control (PC), because MG5 cells express mRNA and protein for GPNMB as previously reported (Kawahara et al., 2016). M indicates the molecular markers. (d) Results in (c) were quantified. The values of type 1 MG (−) were set at 1. Full-length western bolts of panel (b) and the antibody validation data are shown in Figures S0–S1 and S0–S2, respectively). Because of low recovery of primary microglial cells from neonatal mouse brain (ca. 3×10^5 cells/brain), large-scale preparation (42 mice) was performed for western blotting analysis in (b) and (c). (e) Primary type 1 MG and type 2 MG from wild-type (WT) mice (columns 1–3, 7–9) and *Gpnmb*-knockout (KO) mice (columns 4–6, 10–12) were incubated for 6 h with 3.0 μg/mL of the pre-chromatography sample of ^{125}I-labeled o-Aβ_{1-42} (>1 kDa) in the presence (+) or absence (−) of fucoidan (100 μg/mL) or CA074Me (5 μM). The amounts of ^{125}I-labeled o-Aβ_{1-42} degradation products were determined. Values represent means ± SD of technical triplicate measurements ($n = 3$). The cells in (e) were obtained from primary-cultured cells of 15 brains of neonatal *Gpnmb*-KO mice and 15 brains of neonatal WT mice. Statistical significance for column 1 or 7 (****$p < 0.0001$ and $p = 0.7235$) and column 4 or 10 (####$p < 0.0001$) were determined using Tukey's multiple comparison test. Additional results are shown in Figures S2–S4).

species of ^{125}I-o-Aβ_{1-42} by a Sephadex G-100 column (1.0 × 24 cm; Figure 3a). The sample of fraction numbers 23–27 (indicated by red lines) were pooled and used as a SEC-isolated ^{125}I-o-Aβ_{1-42}. When compared to the Sephadex G-100 column (1.0 × 47 cm), the column (1.0 × 24 cm) did not separate the ^{125}I-labeled monomer Aβ_{1-42} and free ^{125}I (Figure 1a vs. Figure 3a).

As shown in Figure 3b, the immunocytochemical analysis employing antibodies to GPNMB and Iba1 (a marker of MG) confirmed that the GPNMB protein was not expressed in the type 1 MG deriving from *Gpnmb*-deficient mice (*Gpnmb*-KO MG). In contrast, it was expressed in type 1 MG deriving from wild-type mice (WT MG). Figure 3c shows the endocytic degradation of ^{125}I-o-Aβ_{1-42} by mouse primary type 1 MG in the presence or absence of an excess amount of unlabeled ("cold") o-Aβ_{1-42} (120 μg/mL and 26.6 μM monomer equivalent of total Aβ_{1-42} peptide). The microglial degradation of ^{125}I-o-Aβ_{1-42} took place in a concentration-dependent manner, and the activity was saturated (Figure 3c). In addition, these activities were largely inhibited in the presence of an excess of unlabeled o-Aβ_{1-42}, thereby indicating that this process is receptor-mediated. Importantly, *Gpnmb*-KO MG exhibited a 64% reduction in specific efficacy compared to WT MG (Figure 3c). The apparent K_d of the mouse GPNMB for SEC-isolated o-Aβ_{1-42} (i.e., the degradation activity of WT MG minus those of *Gpnmb*-KO MG) was 0.5 μM monomer equivalent of total Aβ_{1-42} peptide (2.3 μg/mL). In addition, the degradation activity of *Gpnmb*-KO MG was significantly lower than that of WT MG (Figure 3d, column 1 vs. column 7). The o-Aβ_{1-42}-specific, fucoidan-sensitive and CA074Me-sensitive degradation activities were significantly higher in WT MG than those in *Gpnmb*-KO MG (Figures 3d,e). These results indicated that the GPNMB contributes to the o-Aβ_{1-42} clearance undertaken by mouse primary type 1 MG.

Subsequently, we investigated the effect of *Gpnmb* small interfering RNA (siRNA) on o-Aβ clearance activity in mouse microglial cell line MG5 (Figure 4). The transfection of *Gpnmb*-siRNA into MG5 cells significantly reduced the GPNMB expression by 81% (as compared to control siRNA, Figure 4a). The *Gpnmb*-siRNA, as compared to control siRNA, inhibits the degradation of SEC-isolated

^{125}I-o-Aβ_{1-42} by MG5 microglial cells (Figures 4b,c), indicating that GPNMB contributes to the o-Aβ clearance performed by these cells.

3.4 | Cell surface expression of truncated GPNMB in rat primary type 1 MG

GPNMB is known to be expressed not only on endosomes/lysosomes but also on the cell surface (Biondini et al., 2022). Therefore, we investigated whether the GPNMB expressed on the cell surface may be involved in the MG-mediated o-Aβ clearance. We have previously generated the anti-microglial monoclonal antibody 9F5 by immunizing mice with primary-cultured rat type 1 MG (Kawahara et al., 2016). Monoclonal antibodies against macrophages obtained by immunization with macrophages recognize macrophage cell surface proteins often and suppress their function (e.g., Tim4; Miyanishi et al., 2007). We investigated whether the 9F5 antibody could recognize the cell surface protein of MG and suppress their function.

Flow cytometric analysis revealed that the 9F5 antibody recognized the cell surface expression of truncated GPNMB in rat primary type 1 MG (Figure 5Aa), whereas AF2330 [a polyclonal antibody recognizing both full-length and the truncated GPNMB in cell homogenates of rat type 1 MG by immunoprecipitation and western blot analyses (Kawahara et al., 2016)] did not recognize the cell surface expression of GPNMB (Figure 5Ab). These results indicate that 9F5 but not AF2330 is a suitable antibody for flow cytometric analysis and that 9F5 but not AF2330 recognizes the native form of truncated GPNMB on the cell surface.

Mouse GPNMB (also known as DC-HIL) mostly localizes in the cytoplasm but is present at lower levels on the surface of XS52 dendritic cells (Shikano et al., 2001). We were unable to determine the cell surface expression of full-length GPNMB in rat primary type 1 MG using a biochemical method because the cells showed cytotoxicity during treatment with biotin-(AC$_5$)$_2$ Sulfo-OSu (0.5 mg/mL in phosphate buffered saline [PBS]; Dojindo) at 4°C for 60 min (data not shown). In addition, we tried to use an anti-mouse GPNMB antibody (CTSREVL,
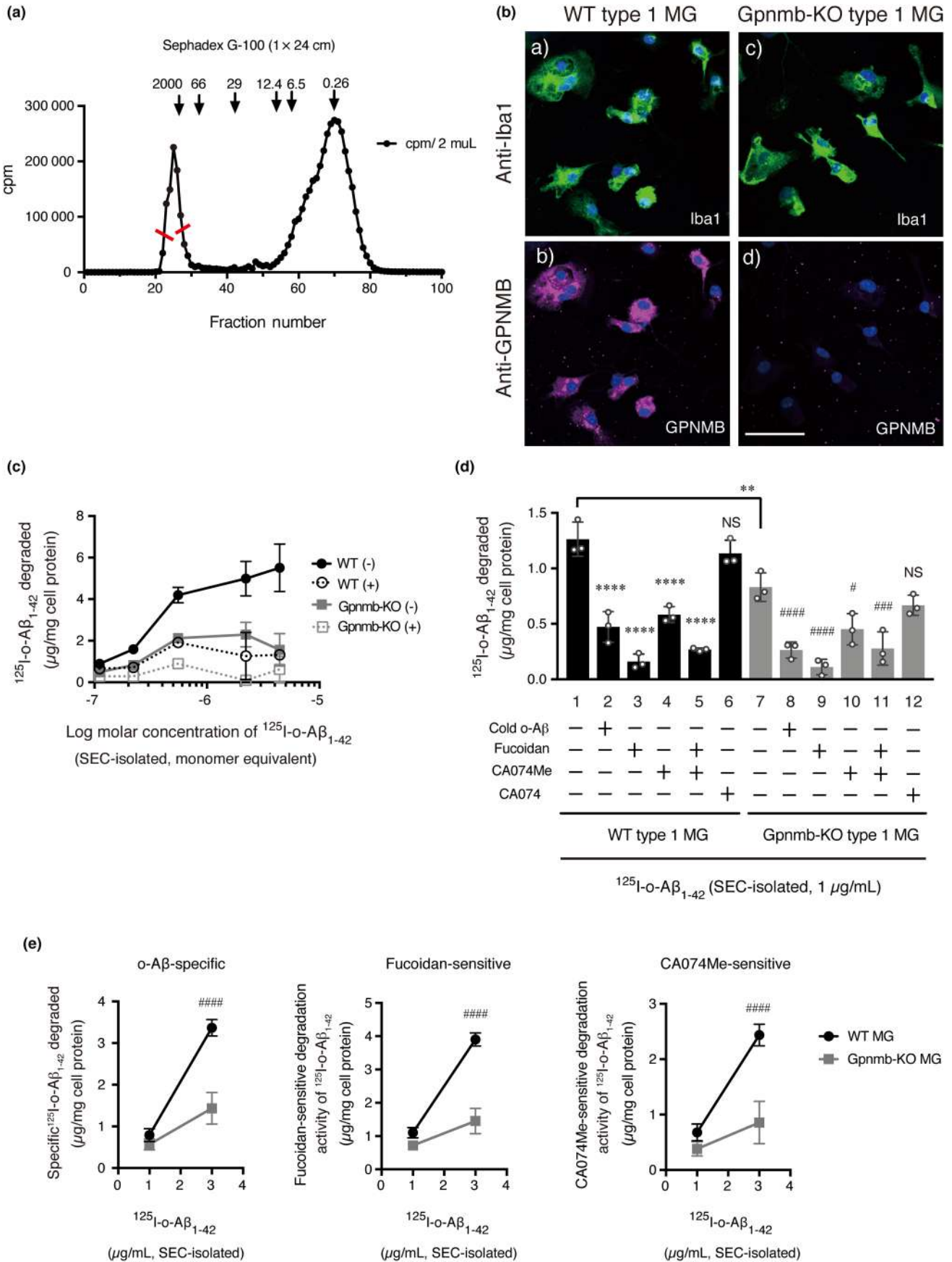
(a)

(b)

(c)

(d)

(e)

FIGURE 3 Comparison of the endocytosis of SEC-isolated o-Aβ_{1-42} delivered by primary type 1 MG deriving from *Gpnmb*-knockout mice with that delivered by cells deriving from wild-type mice. (a) Preparation of SEC-isolated ^{125}I-labeled o-Aβ_{1-42}. ^{125}I-labeled o-Aβ_{1-42} (451.5 μg) was chromatographed on a Sephadex G-100 column (1.0×24 cm) and was fractionated per 0.33 mL each. The radioactivity of 2-μL aliquots from each fraction was determined by using a γ-counter. The gel-included broad peak elutes at ca. 23 mL (fraction number 70), while the gel-excluded peak elutes at ca. 8.3 mL (fraction number 25). The samples of fraction numbers 23–27 (indicated by red lines) were pooled and used as an SEC-isolated ^{125}I-labeled o-Aβ_{1-42} (specific activity: 427 cpm/ng; % free: 1.9%). Arrows indicate elution positions of the molecular weight standards. Molecular masses are indicated in kDa. (b) Primary type 1 MG from wild-type (WT) mice (a, b) and from *Gpnmb*-knockout (KO) mice (c, d) were stained with an anti-Iba1 (a, c) or an anti-GPNMB (AF2330; b, d) antibody. Nuclei were stained with Hoechst 33258. Bar: 50 μm. (c) Mouse WT and *Gpnmb*-KO type 1 MG were incubated for 6 h with the indicated concentrations (0.5, 1, 2.5, 10, and 20 μg/mL) of SEC-isolated ^{125}I-labeled o-Aβ_{1-42}, in the presence (+) or absence (−) of an excess amount of unlabeled ("cold") o-Aβ_{1-42} (120 μg/mL), and then, the amounts of degradation products of ^{125}I-labeled o-Aβ_{1-42} were determined. Values represent mean ± range ($n=2$), and data are representative of two independent biological experiments. (d) Mouse WT and *Gpnmb*-KO type 1 MG were incubated for 6 h with 1 μg/mL of SEC-isolated ^{125}I-labeled o-Aβ_{1-42} in the presence or absence of cold o-Aβ_{1-42} (120 μg/mL), fucoidan (100 μg/mL), CA074Me (5 μM), or CA074 (5 μM). The amounts of the degradation products of the ^{125}I-labeled o-Aβ_{1-42} were determined. Values represent the mean ± SD ($n=3$), and additional results are shown in Figure S5. Statistical significances (**$p < 0.01$, ****$p < 0.0001$, and non-significant; NS) for column 1 were determined by Tukey's multiple comparison test, and so where those for column 7 ($^{#}p < 0.05$, $^{###}p < 0.001$, $^{####}p < 0.0001$, and NS). (e) The o-Aβ_{1-42}-specific, the fucoidan-sensitive, and the CA074Me-sensitive degradation products in WT and *Gpnmb*-KO type 1 MG were shown. Values represent the mean ± SD ($n=3$). Statistical significances ($^{####}p < 0.0001$) were determined by Bonferroni multiple comparison test following two-way ANOVA.

#50-5708-80, Thermo Fisher Scientific) for flow cytometric analysis, but we were unable to observe positive signal in mouse microglial MG5 cells (data not shown). Given the commercial unavailability of an antibody that recognizes the native form of full-length GPNMB on the cell surface, we focused on the function of truncated GPNMB expressed on the cell surface in the present study.

Confocal microscopy revealed that the antigen for 9F5, a truncated GPNMB, was colocalized with Aβ_{1-42} in rat primary type 1 MG following o-Aβ_{1-42}-induced stimulation for 2 h (Figure 5Ba,b). In addition, the antigen for AF2330 (an antibody recognizing both full-length and the truncated GPNMB) and Aβ_{1-42} was colocalized following o-Aβ treatment for 2 h (Figure 5Bc,d). These results suggest that GPNMB protein, including the truncated form, may interact with Aβ_{1-42} within the cells at 2 h after o-Aβ treatment.

3.5 | Truncated GPNMB serves as a scavenger receptor for o-Aβ in rat primary type 1 MG

Because 9F5 recognizes the cell surface truncated GPNMB and the antigen was colocalized with Aβ_{1-42} within the cells following o-Aβ treatment (Figure 5), we investigated whether 9F5 would inhibit the binding and uptake process of ^{125}I-o-Aβ_{1-42} in these cells. The specific association and degradation, obtained by subtracting the non-specific activity from the total activity, yielded a saturation pattern (Figures 6a,c). On the other hand, 9F5 inhibited the specific cell-association and degradation activities of ^{125}I-o-Aβ_{1-42} by rat primary type 1 MG by 52% and 51%, respectively (Figure 6b,d; Figure S7). Its inhibition mode developed in a non-competitive manner, suggesting that there might be two mechanisms involved. Firstly, the 9F5 may suppress the o-Aβ clearance by internalizing the truncated GPNMB. Secondly, the 9F5 may indirectly suppress the activity of the unknown protein required for the Aβ clearance by binding to the truncated GPNMB.

In order to evaluate whether the truncated GPNMB functions as a receptor for o-Aβ, we attempted to determine the cellular binding of

^{125}I-o-Aβ_{1-42} to rat primary type 1 MG, at 4°C, for 90 min (Figure 6e,f). The total binding of ^{125}I-o-Aβ_{1-42} was inhibited by 42% by an excess amount of unlabeled o-Aβ_{1-42}, and by 52% by 9F5 antibody, but not by control mIgG$_1$. The 9F5 antibody inhibited the binding of ^{125}I-o-Aβ_{1-42} to rat primary type 1 MG in a dose-dependent manner. When the incubation of o-Aβ with rat type 1 MG was carried out at 37°C for 90 min, the total uptake activity was increased by about fivefold compared with the treatment at 4°C (Figure 6g, column 1 vs. Figure 6f, column 1), and the process was partially inhibited by 9F5 (Figure 6g). This result indicates that the o-Aβ uptake process is temperature-dependent and that the truncated GPNMB contributes to this temperature-sensitive phagocytosis (Goldstein et al., 1983).

As 9F5 antibody does not react to mouse MG (Kawahara et al., 2016), the effect of 9F5 antibody on the Aβ clearance in mouse type 1 MG was investigated as a negative control. As a result, 9F5 antibody did not affect Aβ clearance in mouse type 1 MG (Figure 6h). We confirmed that the degradation of ^{125}I-o-Aβ_{1-42} was blocked when the intact cells were incubated with an inhibitor of lysosomal function, such as bafilomycin A1 (Figure 6h).

3.6 | o-Aβ_{1-42} interacts with GPNMB proteins including antigen for 9F5 in rat primary type 1 MG

To confirm our finding that o-Aβ_{1-42} directly binds to truncated GPNMB (as shown in Figures 6e,f), we performed the other cell-based binding assays.

We performed co-immunoprecipitation experiments using 9F5 antibody and anti-Aβ antibody in rat primary type 1 MG. However, we were unable to investigate the interaction because (1) the extraction efficiency of o-Aβ_{1-42} from the cells was low, and (2) the epitope of 9F5 on GPNMB may be masked with o-Aβ_{1-42} as suggested in Figure 6e,f (Figures S9 and S10).

We observed that one of the high molecular weight GPNMB proteins (ca. 80 kDa) was immunoprecipitated by 9F5 antibody
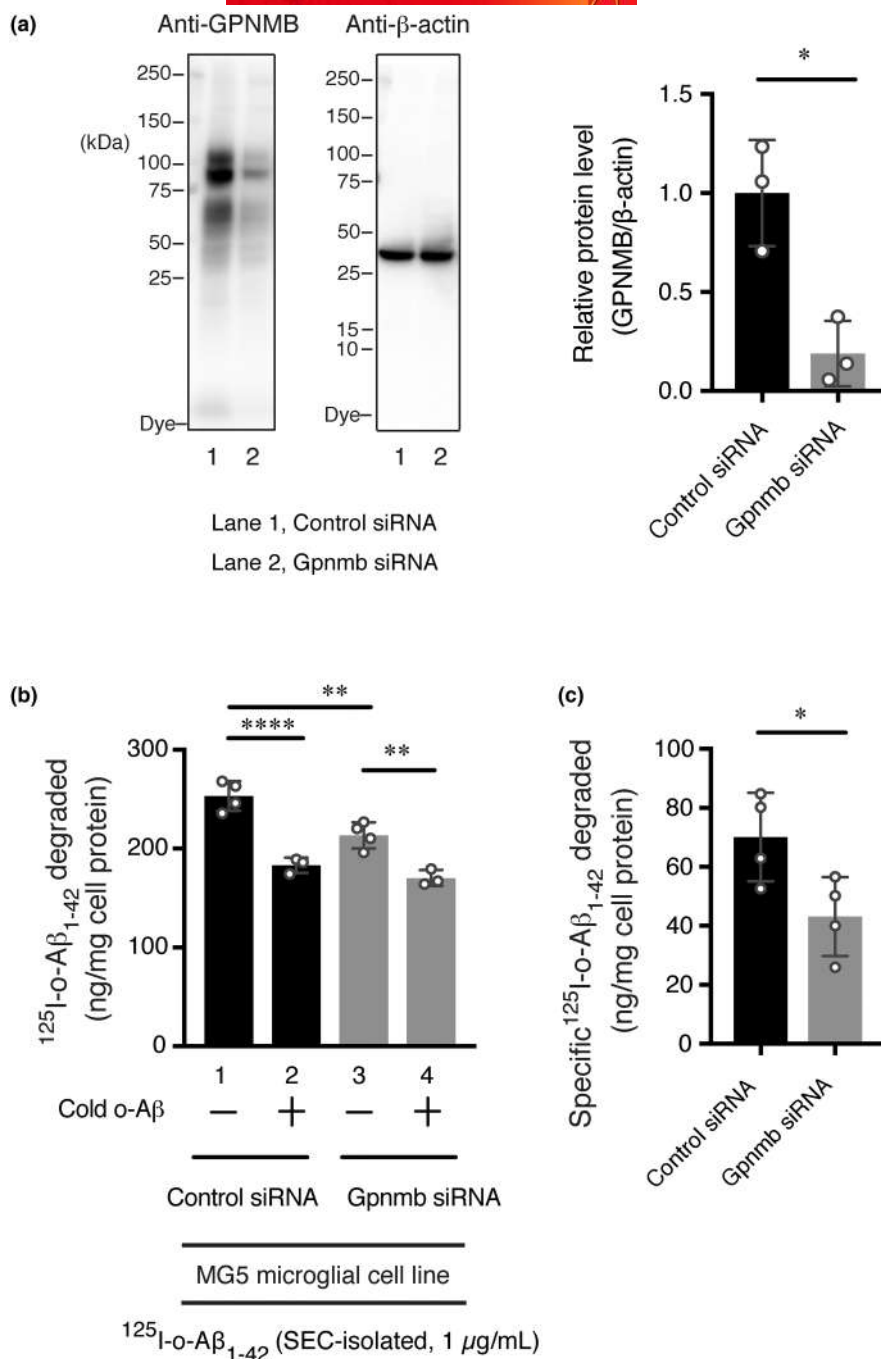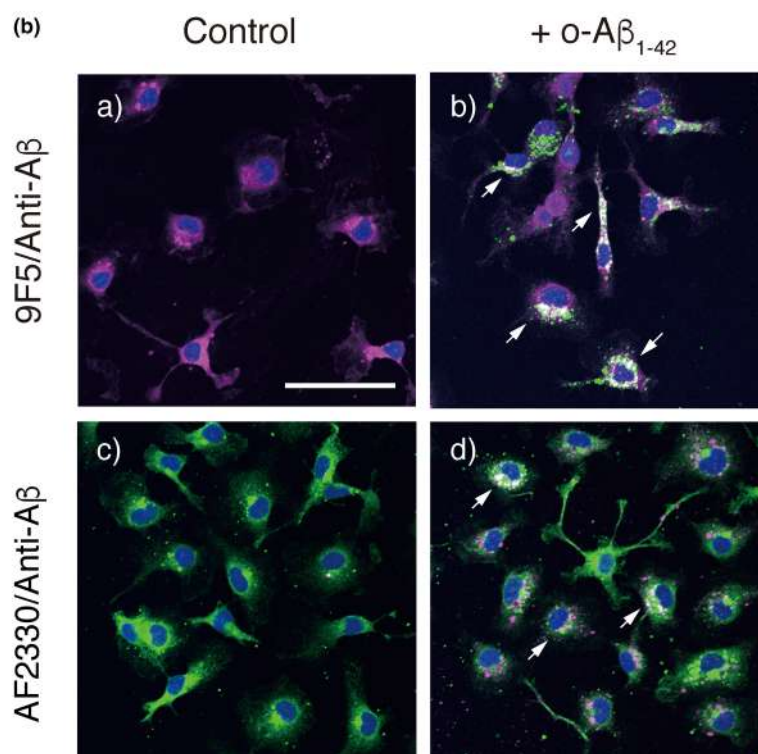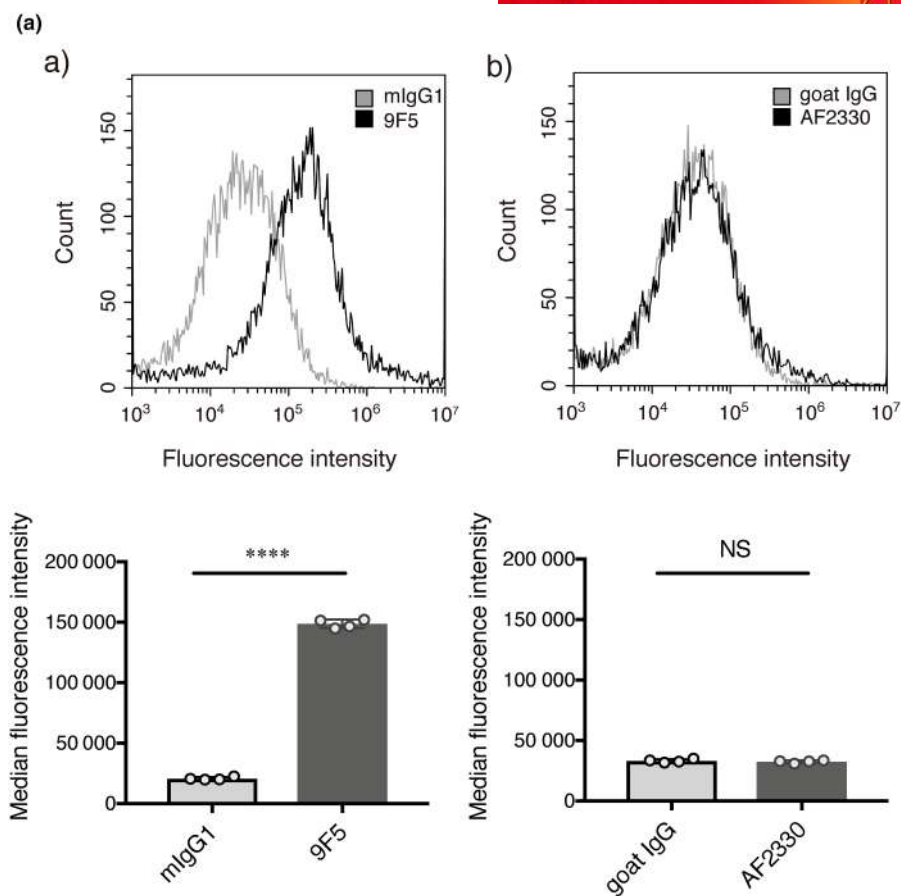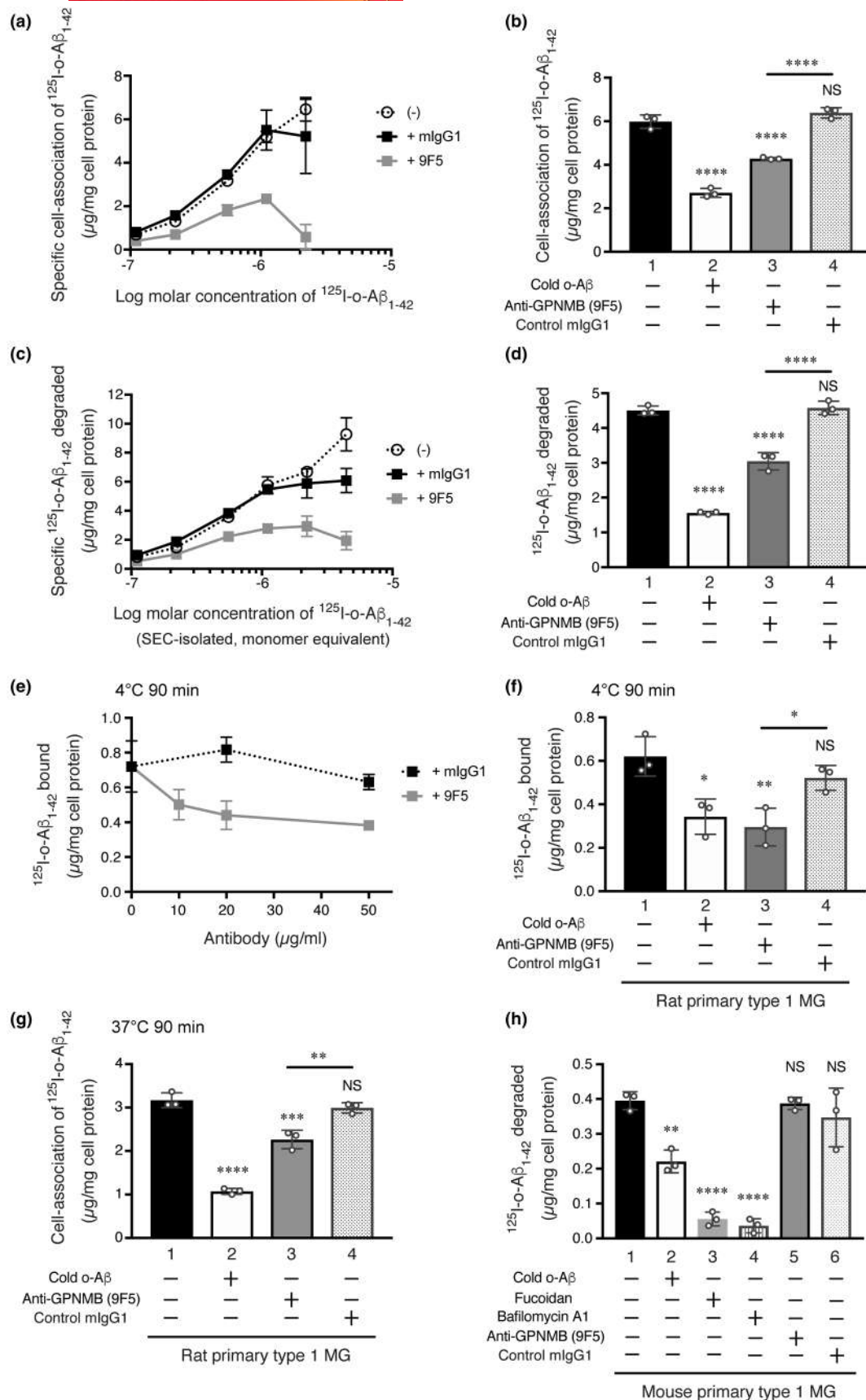
(a)

Anti-GPNMB   Anti-β-actin

Lane 1, Control siRNA
Lane 2, Gpnmb siRNA

(b)

Cold o-Aβ   − + − +

Control siRNA   Gpnmb siRNA

MG5 microglial cell line

^{125}I-o-Aβ$_{1-42}$ (SEC-isolated, 1 μg/mL)

(c)

FIGURE 4 A *Gpnmb*-siRNA inhibits the degradation of SEC-isolated o-Aβ$_{1-42}$ by murine microglial MG5 cells. Murine MG5 cells were transfected with control siRNA or *Gpnmb*-siRNA. (a) At 72 h after transfection, the cell lysates (30 μg) were subjected to immunoblotting analysis for GPNMB and β-actin. Lane 1, control siRNA. Lane 2, Gpnmb-siRNA. Data are representative of three independent experiments. Results were quantified, and maximal values were set at 1. Values represent the mean ± SD ($n = 3$). Statistical significances (*$p < 0.05$) were determined by Student's *t*-test. Full-length western bolts of panel (a) are shown in Figure S0–S3). (b) At 72 h after transfection, the cells were incubated for 6 h with 1 μg/mL of SEC-isolated ^{125}I-labeled o-Aβ$_{1-42}$, in the presence or absence of cold o-Aβ$_{1-42}$ (120 μg/mL). The amounts of the degradation products of the ^{125}I-labeled o-Aβ$_{1-42}$ were determined. Values represent the mean ± SD ($n = 3$–4). Statistical significances (**$p < 0.01$ and ****$p < 0.0001$ for column 1, and **$p < 0.01$ for column 3) were determined by Tukey's multiple comparison test. (c) The specific degradation products in (b) were shown. Values represent the mean ± SD ($n = 3$–4). Statistical significances (*$p < 0.05$) were determined by Student's *t*-test.

FIGURE 5 The 9F5 antibody, but not AF2330, recognizes the native form of truncated GPNMB on the cell surface of rat primary type 1 MG. (a) Rat primary type 1 MG were incubated with 9F5 (a mouse anti-truncated GPNMB monoclonal antibody) and an Alexa Fluor 488-labeled goat anti-mouse IgG (a) or with AF2330 (goat anti-GPNMB polyclonal antibody) and an Alexa Fluor 488-labeled donkey anti-goat IgG (b), and were subsequently analyzed on a fluorescence-activated cell sorter. Cell populations observed are shown (black line). Stained results with control IgG are also shown (gray line). Lower panels show quantitative comparison of median fluorescence intensity of 9F5+ cells, mIgG1+ cells, AF2330+ cells, and goat IgG+ cells in rat type 1 MG. Values represent mean ± SD ($n = 4$ of technical replicates), and data are representative of three independent biological experiments. Statistical significances (****$p < 0.0001$, and NS) were determined by Student's *t*-test. Antibody validation data were shown in Figure S0–S4. (b) The cellular localization of the GPNMB protein after an o-Aβ$_{1-42}$-induced stimulation in rat type 1 MG. Rat type 1 MG were cultured for 2 h in MEM containing 10% FBS in the presence (b, d) or absence (a, c) of o-Aβ$_{1-42}$ (1 μg/mL), and were then double-stained with a mouse anti-truncated GPNMB antibody (9F5; a, b) and a rabbit anti-Aβ antibody (D54D2; a, b), or a goat anti-GPNMB antibody (AF2330; c, d) and a mouse anti-Aβ antibody (6E10; c, d). Bar: 50 μm. Arrows indicate representative of the intense signal for colocalization of GPNMB with Aβ$_{1-42}$. Data are representative of three independent experiments.

(a)

(b) Control — + o-Aβ$_{1-42}$

1330 | WILEY — Journal of Neurochemistry — JNC *The Official Journal of the International Society for Neurochemistry*

KAWAHARA ET AL.

(Figure S9a), suggesting that the full-length GPNMB (ca. 80 kDa) and truncated GPNMB make a complex. This result was consistent with our previous report that a full-length GPNMB (ca. 89 kDa) and truncated GPNMB (ca. 60 kDa) were co-immunoprecipitated by 9F5

FIGURE 6 The anti-truncated GPNMB antibody 9F5 inhibits the binding, uptake, and degradation of the SEC-isolated ^{125}I-o-Aβ_{1-42} by rat primary type 1 MG. (a, c) Rat primary type 1 MG were incubated for 6 h with the indicated concentrations (0.5, 1, 2.5, 5, and 10 μg/mL) of the SEC-isolated ^{125}I-labeled o-Aβ_{1-42} (a) or with the indicated concentrations (0.5, 1, 2.5, 5, 10, and 20 μg/mL) of the SEC-isolated ^{125}I-labeled o-Aβ_{1-42} (c) in the presence (+) or absence (−) of 9F5 (20 μg/mL) or control mIgG$_1$ (20 μg/mL). The amounts of the specific cell-association (a) and the specific degradation products (c) of the ^{125}I-labeled o-Aβ_{1-42} were determined. Non-specific cell-association/degradation measurements were determined in the presence of the appropriate ^{125}I-ligand and excess amount of unlabeled ligand (o-Aβ_{1-42}, 120 μg/mL). These nonspecific values were subtracted from the total cell-association/degradation to establish the specific cell-association/degradation. Values represent the mean ± range of duplicate measurements, and additional results are shown in Figure S6. (b, d) Rat type 1 MG were incubated for 6 h with 1.8 μg/mL of SEC-isolated ^{125}I-labeled o-Aβ_{1-42} in the presence or absence of cold o-Aβ_{1-42} (120 μg/mL), 9F5 (50 μg/mL), or mIgG$_1$ (50 μg/mL). The amounts of the cell-association (b) and the degradation products (d) of the ^{125}I-labeled o-Aβ_{1-42} were determined as described. Values represent the mean ± SD ($n=3$ of technical replicates), and data are representative of at least two independent biological experiments. The concentration of ^{125}I-o-Aβ_{1-42} (1.8 μg/mL) was selected from the results of dose–response curve (a and c). Additional results are shown in Figure S7. (e) Rat type 1 MG were incubated at 4°C, for 90 min, with 3 μg/mL of SEC-isolated ^{125}I-labeled o-Aβ_{1-42}, in the presence or absence of the indicated concentrations (10, 20, and 50 μg/mL) of 9F5 or the indicated concentrations (20, 50 μg/mL) of mIgG$_1$. The amount of binding of the ^{125}I-labeled o-Aβ_{1-42} was determined. Values represent the mean ± SD ($n=3$). Additional results are shown in Figure S8. (f) Rat type 1 MG were incubated at 4°C, for 90 min, with 1.5 μg/mL of SEC-isolated ^{125}I-labeled o-Aβ_{1-42}, in the presence or absence of cold o-Aβ_{1-42} (120 μg/mL), 9F5 (20 μg/mL), or mIgG$_1$ (20 μg/mL). The amount of binding of the ^{125}I-labeled o-Aβ_{1-42} was determined. Values represent the mean ± SD ($n=3$). (g) Rat type 1 MG were incubated at 37°C, for 90 min, with 1.5 μg/mL of SEC-isolated ^{125}I-labeled o-Aβ_{1-42}, in the presence or absence of cold o-Aβ_{1-42} (120 μg/mL), 9F5 (50 μg/mL), or mIgG$_1$ (50 μg/mL). The amounts of the cell-association products of the ^{125}I-labeled o-Aβ_{1-42} were determined. Values represent the mean ± SD ($n=3$). (h) Mouse primary type 1 MG were incubated at 37°C, for 6 h, with 1.5 μg/mL of SEC-isolated ^{125}I-labeled o-Aβ_{1-42}, in the presence or absence of cold o-Aβ_{1-42} (120 μg/mL), fucoidan (100 μg/mL), bafilomycin A1 (0.5 μM), 9F5 (20 μg/mL), or mIgG$_1$ (20 μg/mL). The amounts of the degradation products of the ^{125}I-labeled o-Aβ_{1-42} were determined. Values represent the mean ± SD ($n=3$). Statistical significances (*$p<0.05$, **$p<0.01$, ***$p<0.001$, ****$p<0.0001$, and NS for column 1, and *$p<0.05$, **$p<0.01$, ****$p<0.0001$ and NS for column 4) were determined by Tukey's multiple comparison test.

antibody (Figure 4c of Kawahara et al., 2016). However, it remains unknown whether the full-length GPNMB (ca. 80 kDa) may contribute to the binding of truncated GPNMB to o-Aβ_{1-42}.

Since we observed that 9F5-positive antigen and Aβ were colocalized as shown in Figure 5b, we performed a recently developed proximity ligation method to examine the protein–protein interactions at single-molecule resolution (Söderberg et al., 2006). We confirmed the reproducibility of the colocalization of antigen for 9F5 and AF2330 with Aβ_{1-42} in rat primary type 1 MG following o-Aβ_{1-42}-induced stimulation for 2 h (Figures S11 and S12). Under these conditions, we observed that the Alexa Fluor 594 signal, which appears when Aβ_{1-42} interacts with antigen for 9F5 and AF2330, was increased in o-Aβ_{1-42}-stimulated rat primary type 1 MG (Figure 7). These signals were inhibited by a preincubation with fucoidan (Figure 7). These results indicated that internalized o-Aβ_{1-42} interacts with GPNMB proteins including antigen for 9F5 in rat primary type 1 MG, and the reaction is a fucoidan-sensitive manner.

3.7 | Effect of 9F5 on the degradation of o-Aβ_{1-42} by human-induced pluripotent stem cell (iPSC)-derived MG

We examined the effect of 9F5 on degradation of o-Aβ_{1-42} in human iPSCs-derived MG-like cells. We confirmed that GPNMB proteins including the truncated form are expressed in human iPSCs-derived MG-like cells by western blot analysis (Figure 8a–e). Immunocytochemical analysis also revealed that 9F5 recognizes the human antigen in Iba1-positive MG-like cells from iPSCs (Figure 8f). Human iPSCs-derived MG were incubated with a SEC-isolated

^{125}I-labeled o-Aβ_{1-42} with or without an excess amount of unlabeled o-Aβ_{1-42}, fucoidan, CA074Me, anti-GPNMB antibody (9F5), or control mouse IgG$_1$ (15H6), and subsequently, the degradation products were determined. The degradation activity in the cells was inhibited by excess amount of unlabeled o-Aβ_{1-42}, fucoidan, and CA074Me (Figure 8g). The degradation activity in human MG-like cells was significantly increased by mouse IgG$_1$, but the increased amount of degradation activity was inhibited by 9F5 antibody (Figure 8h). These results suggest that the mouse IgG$_1$/human Fc receptor signaling increases the microglial Aβ clearance. In contrast, 9F5 inhibits the interaction of o-Aβ with GPNMB in human MG-like cells.

We performed immunohistochemical analysis of tissue sections from the hippocampus of brain of patient with AD, finding 9F5-positive cells, Iba1-positive cells, and senile plaques in the sections (Figure S13). However, because the sample size was limited ($n=1$), more extensive studies are needed to determine whether truncated GPNMB-positive MG are abundant in the senile plaques of brain of patients with AD and whether truncated GPNMB protein is highly expressed in these brains.

3.8 | *Gpnmb* deficiency increases the mortality of female APP23 mice, *an AD model*

Finally, in order to investigate the in vivo role of endogenous GPNMB in pathogenesis of AD, we compared the survival curve between APP23;*Gpnmb*$^{+/+}$ and APP23;*Gpnmb*$^{-/-}$ mice. We observed that *Gpnmb* deficiency increased the mortality of female, but not male, APP23 mice (Figure 9). GPNMB+Iba1+ MG around Aβ plaque were observed in brain of 10-month-old female APP23 mice (Figure S14).
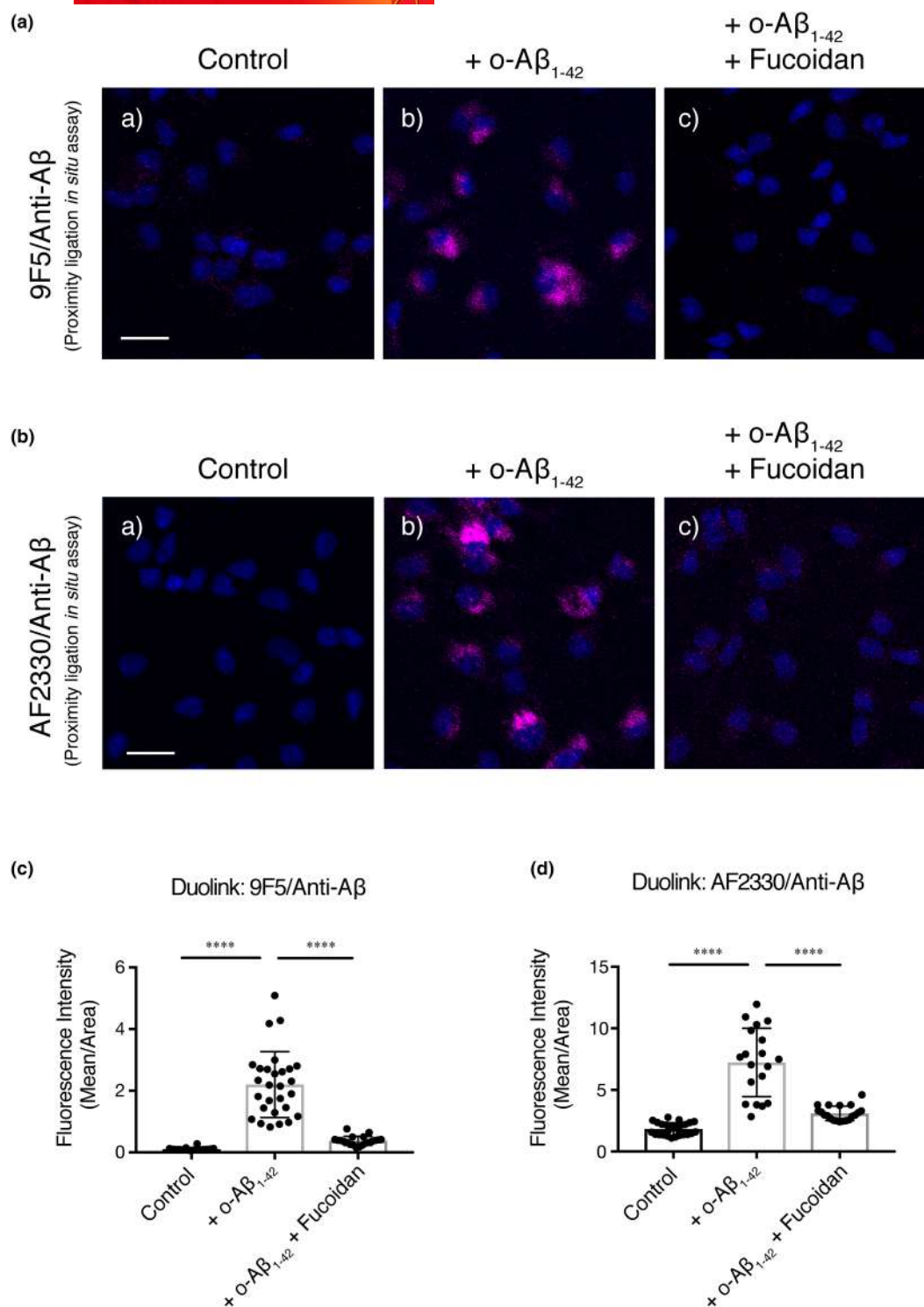
FIGURE 7 Internalized o-Aβ$_{1-42}$ interacts with GPNMB proteins including antigen for 9F5 in rat primary type 1 MG. (a, b) Rat primary type 1 MG were incubated for 30 min in MEM containing 10% FBS in the presence (c) or absence (a, b) of 100 μg/mL of fucoidan, and were then cultured for 2 h in MEM containing 10% FBS in the presence (b, c) or absence (a) of o-Aβ$_{1-42}$ (2 μg/mL). The cells were subjected to proximity ligation in situ assay. (a) A mouse anti-truncated GPNMB antibody (9F5) and a rabbit anti-Aβ antibody (D54D2). (b) A goat anti-GPNMB antibody (AF2330) and a rabbit anti-Aβ antibody (D54D2). Bar: 20 μm. (c, d) The results shown in (a) and (b) were quantified and are given as mean ± SD ($n = 16–28$ in (c); $n = 19–26$ in (d)). Statistical significances (****$p < 0.0001$) were determined by Tukey's multiple comparison test. Additional results were shown in Figures S11 and S12.

In addition, *Gpnmb* deficiency accelerates TBS-soluble, but not TBS-insoluble, $A\beta_{42}$ accumulation of hippocampus in 10-month-old female APP23 mice (Figure S15). We also observed that *Gpnmb* deficiency tended to increase the mortality of female, but not male, 5xFAD mice, another AD model (Figure S16). These results suggest that GPNMB, including the truncated form, may contribute to the $A\beta_{42}$ metabolism in female AD brain. However, it remains unknown why the contribution of GPNMB in an AD model mouse was seen only in females, and further studies are needed in vivo detail.

4 | DISCUSSION

In this study, we found that the truncated GPNMB (the antigen for 9F5) binds to oligomeric form of $A\beta_{1-42}$ and functions as the scavenger receptor. GPNMB is expressed high levels in the cerebrospinal fluid and the brain parenchyma of AD patients (Doroszkiewicz et al., 2023; Hüttenrauch et al., 2018), and possible marker for AD. Our study suggests that GPNMB is one of essential defensive components of AD progression.

4.1 | Role of truncated GPNMB as a scavenger receptor

Analyses using the 9F5 antibody and primary type 1 MG deriving from *Gpnmb*-deficient mice revealed that GPNMB is a molecule that contributes to 52%–64% of the ^{125}I-o-$A\beta_{1-42}$ clearance delivered by primary type 1 MG. In addition, the binding of ^{125}I-o-$A\beta_{1-42}$ to rat primary type 1 MG was inhibited by 52% by the 9F5 antibody. These results indicate that GPNMB contributes to the o-$A\beta_{1-42}$ clearance, and its truncated form functions as a scavenger receptor for o-$A\beta_{1-42}$.

Aβ plays a pivotal role in the progression of AD through its neurotoxic and inflammatory effects (Nakanishi, 2020; Yu & Ye, 2015). On the one hand, Aβ binds to MG, which leads to activation of MG and production of inflammatory mediators. On the other hand, Aβ is cleared by MG through receptor-mediated phagocytosis and degradation. We observed that truncated GPNMB contributes to phagocytosis and clearance of o-Aβ by MG; however, whether truncated GPNMB mediates the production of proinflammatory mediators following the o-Aβ binding remains unknown.

So far, many o-Aβ receptors have been revealed (Yu & Ye, 2015). In particular, *Trem2*, the gene encoding an o-Aβ receptor expressed in MG (Zhao et al., 2018), has been identified as a risk gene for AD pathology (Guerreiro et al., 2013), and therefore, vigorous research is underway regarding this receptor. Since type 1 MG express several o-Aβ receptors including SRA and truncated GPNMB, it is suggested that they function synergistically as scavenger receptors on type 1 MG. It is also known that GPNMB is not expressed in all MG but only in some MG (Kamphuis et al., 2016; Kawahara et al., 2016). Recent detailed studies have revealed that the *Gpnmb* mRNA is strongly expressed in one subtype of MG that appears in the brain in a

Trem2-dependent manner in the late stages of a mouse model of AD (Krasemann et al., 2017; Song et al., 2018). Therefore, it is suggested that in the early stage of AD pathology, TREM2 and others play a central role as receptors for o-Aβ. In contrast, GPNMB, a marker molecule for the disease-associated MG (Friedman et al., 2018; Krasemann et al., 2017), may contribute to the removal of o-Aβ during the late stage of AD. In future research, it is important to perform single-cell RNA sequencing analysis of type 1 and type 2 MG and to compare them with the signatures of disease-associated MG.

The phenotype of *Gpnmb* deficiency in APP23 mice was partially consistent with that of another scavenger receptor, SRA. For example, it is reported that the deficiency of gene for scavenger receptor type A accelerates Aβ accumulation, leading to increased mortality in PS1-APP mice (Frenkel et al., 2013). We observed that deficiency of gene for GPNMB accelerates hippocampal $A\beta_{42}$ accumulation, leading to increased mortality in female APP23 mice. Therefore, it is suggested that GPNMB, including the truncated form, may contribute to the $A\beta_{42}$ metabolism in female AD brain. However, it remains unknown why the contribution of GPNMB in an AD model mouse was seen only in females, and further studies are needed in vivo detail. APP23 mice and 5xFAD mice are transgenic mice that use the Thy1 promoter, which may affect the AD pathogenesis of sex-difference (Sadleir et al., 2015). Therefore, it is necessary to utilize more sophisticated models, such as APP knock-in mice, for analysis of sex-difference.

4.2 | Ligand for GPNMB

In the present study, o-Aβ has been identified as a ligand for GPNMB. Recent reports have shown that GPNMB is up-regulated with the formation of Aβ plaques and tau accumulation (Hales et al., 2016; Lee et al., 2021). It has also been shown that GPNMB increases with the accumulation of α-synuclein in patients with Parkinson's disease (Brendza et al., 2021; Moloney et al., 2018; Zucca et al., 2018). Therefore, it is necessary to investigate whether the oligomeric tau and synuclein also function as ligands for GPNMB. Diaz-Ortiz et al. (2022) showed that human GPNMB interacts with α-synuclein in a cell-based assay, although it remains unclear whether the oligomeric form of α-synuclein interacts with GPNMB. In previous studies, GPNMB was shown to bind to carbon nanotubes (He et al., 2018) and dermatophytes (Chung et al., 2009), but it is not clear whether it functions as a receptor for these substances. Therefore, it is an important task to clarify whether the 9F5 antibody used in this study can block these interactions. In particular, whether GPNMB contributes to the activation of the inflammasome caused by o-Aβ in MG remains an issue, as carbon nanotubes do in macrophages (He et al., 2018). Furthermore, since the antigen for 9F5 is locally expressed in the developing rat brain and in the retinal pigment epithelial cells (Kawahara et al., 2016), we need to elucidate what kind of ligand is recognized and degraded by the truncated GPNMB in these regions.
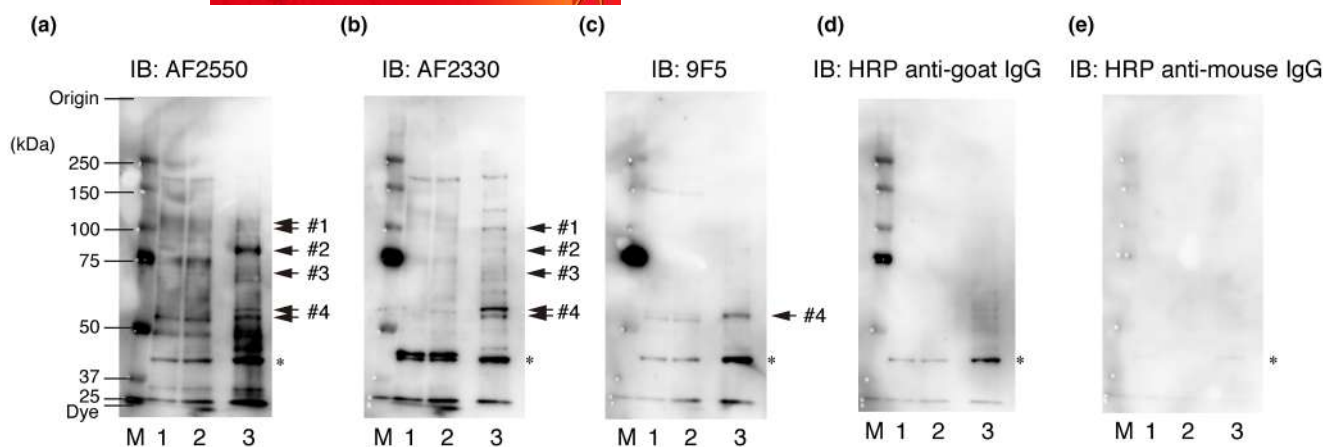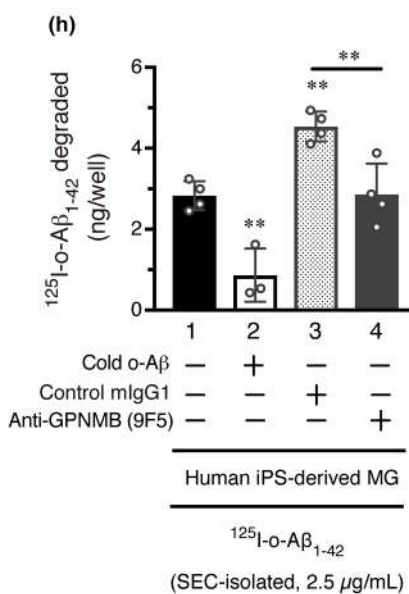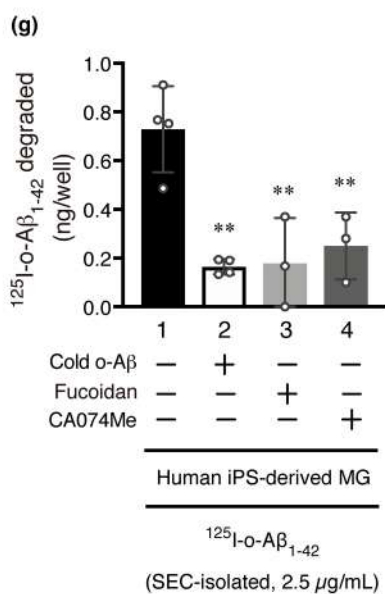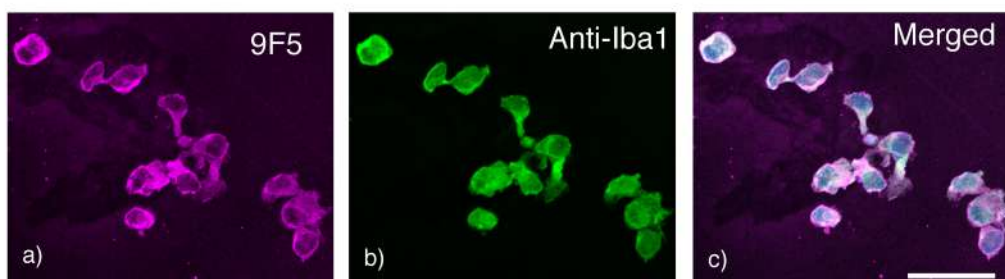
Lane 1, 1% NP-40 extracts of rat primary type 1 MG (non treatment)

Lane 2, 1% NP-40 extracts of rat primary type 1 MG (treated with 2 μg/mL of o-Aβ$_{1-42}$ for 2 h)

Lane 3, Total cell homogenates of human iPS-derived MG-like cells (non treatment)

4.3 | o-Aβ binding site in microglial GPNMB

The three-dimensional structure of the rat GPNMB has not yet been resolved. However, K^{170} seems to be on the protein surface, given the furin-like protease processing at the dibasic motif (K^{169}-K^{170}; Kawahara et al., 2016). When the three-dimensional structure of rat GPNMB was predicted by using the AlphaFold Protein Structure Database (Jumper et al., 2021; https://alphafold.ebi.ac.uk), the dibasic motif (K^{169}-K^{170}) was at the surface (Figure 10; Figures S17 and S18). Interestingly, the surface of rat truncated GPNMB in near K^{170} was predicted to have a lot of basic amino acid residues (Figure 10d) that may be responsible for the

FIGURE 8 The 9F5 antibody, as compared with the isotype-matched control mIgG$_1$, inhibits the degradation of the SEC-isolated o-Aβ_{1-42} by MG-like cells deriving from human iPSCs. (a–e) Western blot analysis of GPNMB proteins in human iPSCs-derived MG-like cells. Human iPSCs-derived MG-like cells (6×10^4 cells/well in 96-well plate) were washed twice with ice-cold PBS and scraped with 15 μL/well of sampling buffer for SDS-PAGE. The total cell homogenates (20 μL) were incubated at 70°C for 10 min and were then subjected to immunoblot analysis with antibodies against GPNMB (a, AF2550; b, AF2330; c, 9F5). The cell lysates (2.5 μg; an extract with TBS containing 1% NP-40) from rat type 1 MG that were (lane 2) or were not (lane 1) treated with 2 μg/mL of o-Aβ_{1-42} for 2 h were used as a positive control for the immunoblotting. The PVDF membrane in (a) was reproved with 9F5 antibody (c) and was then reproved with AF2330 antibody (b). The membrane was also incubated with HRP anti-mouse IgG (e) and HRP anti-goat IgG (d). Mouse TrueBlot ULTRA Anti-Mouse Ig HRP (#18-8817-31, Rockland Immunochemicals, Inc.) was used in (c) and (e). M indicates the molecular markers. The antibody validation data are shown in Figures S0–S5 and S0–S6). (f) MG-like cells deriving from human iPSCs were stained with the 9F5 (a) or with an anti-Iba1 (b) antibody. A fluorescent image is shown after merging (c). Nuclei were stained with Hoechst 33258 (c). A bright-field image is also shown in (b). Bar: 50 μm. (g, h) Human iPSCs-derived MG were incubated for 6 h with 2.5 μg/mL of SEC-isolated ^{125}I-labeled o-Aβ_{1-42}, in the presence or absence of cold o-Aβ_{1-42} (120 μg/mL), fucoidan (100 μg/mL), CA074Me (5 μM), anti-GPNMB antibody (9F5; 20 μg/mL), or control mouse IgG$_1$ (15H6; 20 μg/mL). Subsequently, the amounts of the degradation products (d, e) of the ^{125}I-labeled o-Aβ_{1-42} were determined. The degradation activity was indicated as ng/well and is based on the activity recorded from 6.0×10^4 cells in each well. Values represent the mean ± SD ($n = 3$–4). Statistical significances (**$p < 0.01$ for column 1 as well as for column 4; g, h) were determined by Tukey's multiple comparison test.
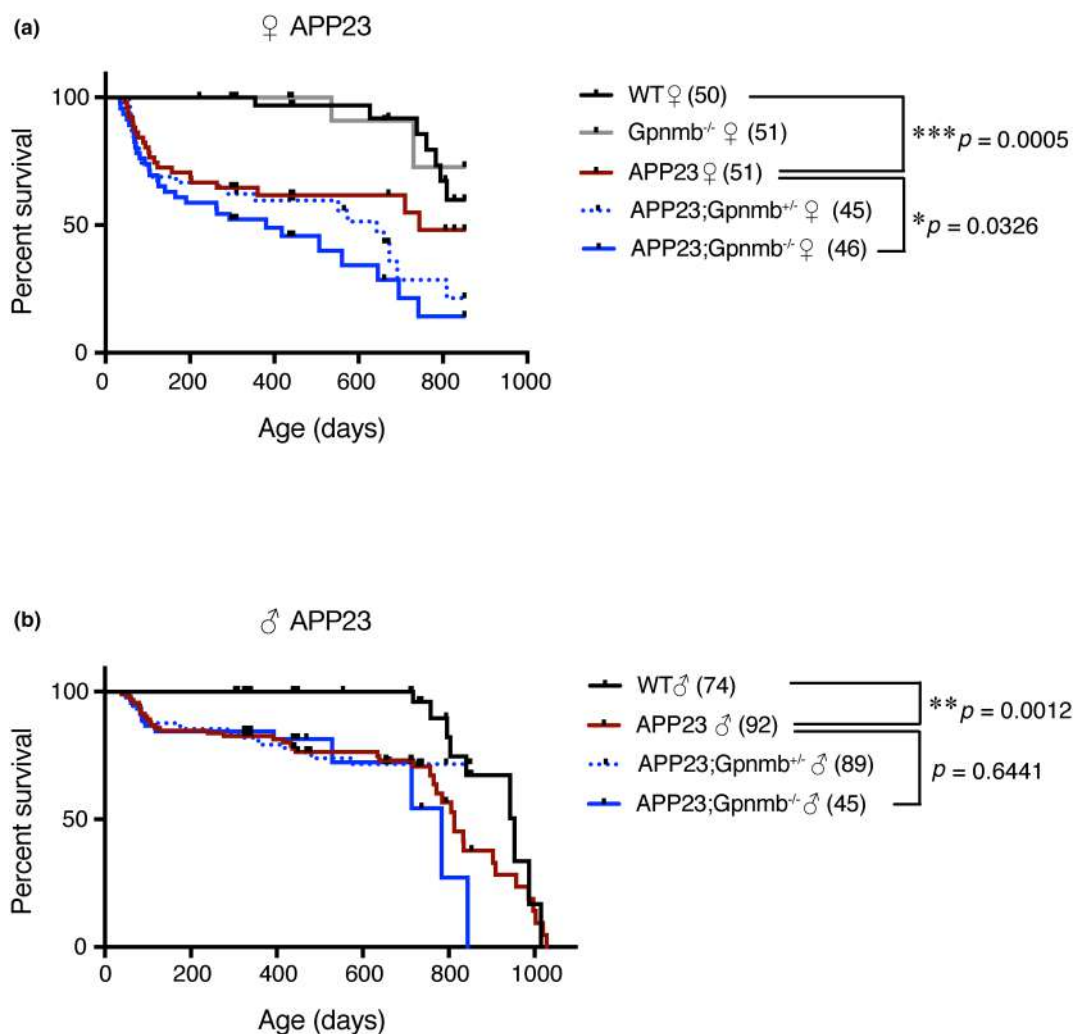

FIGURE 9 Effect of *Gpnmb* gene on survival curves of APP23 mice, an AD model. (a) Female mice. Comparison of survival curves of WT ($n = 50$), *Gpnmb*$^{-/-}$ ($n = 51$), APP23;*Gpnmb*$^{+/+}$ ($n = 51$), APP23;*Gpnmb*$^{+/-}$ ($n = 45$), and APP23;*Gpnmb*$^{-/-}$ ($n = 46$). (b) Male mice. Comparison of survival curves of WT ($n = 74$), APP23;*Gpnmb*$^{+/+}$ ($n = 92$), APP23;*Gpnmb*$^{+/-}$ ($n = 89$), and APP23;*Gpnmb*$^{-/-}$ ($n = 45$). ***$p < 0.001$, **$p < 0.01$, and *$p < 0.05$ by Log-rank (Mantel–Cox) test. Additional results are shown in Figures S14–S16.
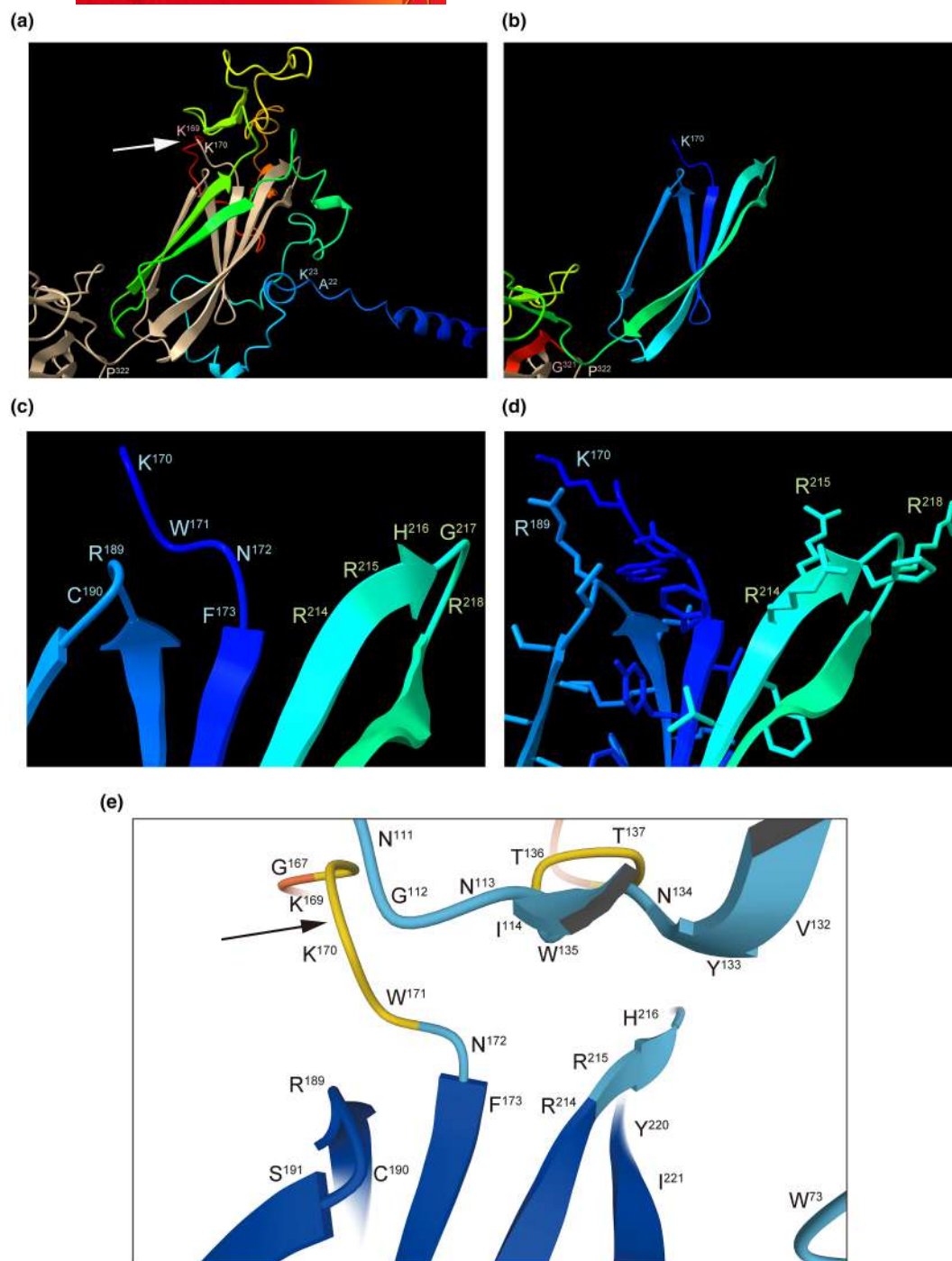
FIGURE 10 A three-dimensional structure of the rat GPNMB, as constructed by AlphaFold2. The protein structure prediction of the rat GPNMB was obtained from the AlphaFold Protein Structure Database, which was developed by DeepMind (UK) and EMBL-EBI (UK; https:// alphafold.ebi.ac.uk/entry/Q6P7C7), updated in AlphaFold DB version at June 1, 2022, and created with the AlphaFold Monomer v2.0. Pipeline. The 3D viewer made the visualization of the database (e), or by using UCSF ChimeraX version 1.4 developed by the UCSF Resource for Biocomputing, Visualization, and Informatics (a–d). Arrow (in a and e) indicates cleavage site by furin-like proteases. Residues 1–169 (in a) and residues 170–321 (in b–d) were colored by rainbow. The distance between the N^{172} and the H^{216} was estimated by the UCSF ChimeraX 1.4 at 7~8 Å. Additional results are shown in Figures S17 and S18.

fucoidan-sensitive binding site for o-Aβ. In the vicinity of these regions, it was existed the CAF domain, which is rich in hydrophobic residues that is required to form physiological amyloid (Pmel17; Hee et al., 2017). Therefore, it was suggested that the CAF domain of GPNMB also constitutes the binding site of o-Aβ via

hydrophobic interaction. The prediction of the three-dimensional structure suggests that the CAF domain of rat GPNMB is covered by its N-terminal domain, and it is not exposed on the cell surface (Figure 10a vs. 10b). Importantly, 9F5 does not react to the full-length GPNMB and specifically recognizes the truncated form of

GPNMB that starts at K^{170}. Therefore, the GPNMB cleaved by a furin-like protease might expose the o-Aβ binding site (including the CAF domain) to the cell surface and interacts efficiently with o-Aβ; however, the interaction is blocked by 9F5 antibody. The epitope structure of 9F5 antibody should be solved experimentally shortly.

We observed that one of the full-length GPNMB (ca. 80 kDa) make a complex with truncated GPNMB (Figure S9a). This result suggests that the full-length GPNMB (ca. 80 kDa) may also bind to o-Aβ$_{1-42}$ without GPNMB truncation. However, because of the lack of specific inhibitors for full-length GPNMB (e.g., the blocking antibody that recognizes native form of full-length GPNMB on the cell surface), we were unable to investigate the contribution of full-length GPNMB to the binding of o-Aβ$_{1-42}$ to rat primary type 1 MG. We would like to analyze in more detail the interaction between o-Aβ$_{1-42}$ and GPNMB by using recombinant proteins in future research.

In the future, it will be necessary to prepare various fragments of the GPNMB (including the CAF domain) and to clarify which exact domain constitutes the o-Aβ binding site. In addition, it will be necessary to clarify the binding mode of the o-Aβ with the GPNMB in detail by performing an epitope analysis of the 9F5 and to investigate whether 9F5 antibody block the interaction between truncated GPNMB and o-Aβ in vivo, as therapeutic potential utilizing this antibody.

In conclusion, we observed that the GPNMB contributes to the o-Aβ$_{1-42}$ clearance and that its truncated form functions as a scavenger receptor for o-Aβ$_{1-42}$ in type 1 MG.

AUTHOR CONTRIBUTIONS

Kohichi Kawahara: Conceptualization; methodology; validation; formal analysis; investigation; resources; writing – original draft; writing – review and editing; visualization; supervision; project administration; funding acquisition. **Takuya Hasegawa:** Formal analysis; investigation; writing – review and editing. **Noa Hasegawa:** Formal analysis; investigation. **Taisei Izumi:** Formal analysis; investigation. **Koji Sato:** Resources; writing – review and editing. **Toshiyuki Sakamaki:** Resources; writing – review and editing. **Masayuki Ando:** Resources; writing – review and editing. **Takehiko Maeda:** Formal analysis; resources; writing – review and editing; project administration.

ACKNOWLEDGMENTS

CONFLICT OF INTEREST STATEMENT

The first author K. K. holds a patent related to the antibody 9F5 (Japan Patent P4815610, 2011-09-09). The *Gpnmb*-knockout mouse is a material co-developed with Daiichi Sankyo Co. Ltd as part of a project (TaNeDS, 2012–2014). This company has no role in this manuscript's interpretation, writing, or publication. The other authors note no conflict of interest to declare.

PEER REVIEW

The peer review history for this article is available at https://www.webofscience.com/api/gateway/wos/peer-review/10.1111/jnc.16078.

DATA AVAILABILITY STATEMENT

The data that support the findings of this study are available from the corresponding author upon reasonable request. Furthermore, information and requests for resources and reagents should be directed to: kkawa@nupals.ac.jp.

ORCID

Kohichi Kawahara https://orcid.org/0000-0003-3195-6649
Takehiko Maeda https://orcid.org/0000-0002-3184-0999

REFERENCES

Biondini, M., Kiepas, A., El-Houjeiri, L., Annis, M. G., Hsu, B. E., Fortier, A. M., Morin, G., Martina, J. A., Sirois, I., Aguilar-Mahecha, A., Gruosso, T., McGuirk, S., Rose, A. A. N., Tokat, U. M., Johnson, R. M., Sahin, O., Bareke, E., St-Pierre, J., Park, M., … Siegel, P. M. (2022). HSP90 inhibitors induce GPNMB cell-surface expression by modulating lysosomal positioning and sensitize breast cancer cells to glembatumumab vedotin. *Oncogene*, *41*, 1701–1717.

Brendza, R., Lin, H., Stark, K., Foreman, O., Tao, J., Pierce, A., Ngu, H., Shen, K., Easton, A. E., Bhangale, T., Chang, D., Bingol, B., & Friedman, B. A. (2021). Genetic ablation of Gpnmb does not alter synuclein-related pathology. *Neurobiology of Disease*, *159*, 105494.

Chrystal, P. W., Footz, T., Hodges, E. D., Jensen, J. A., Walter, M. A., & Allison, W. T. (2021). Functional domains and evolutionary history of the PMEL and GPNMB family proteins. *Molecules*, *26*, 3529.

Chung, J.-S., Sato, K., Dougherty, I. I., Cruz, P. D., Jr., & Ariizumi, K. (2007). DC-HIL is a negative regulator of T lymphocyte activation. *Blood*, *109*, 4320–4327.

Chung, J.-S., Yudate, T., Tomihari, M., Akiyoshi, H., Cruz, P. D., Jr., & Ariizumi, K. (2009). Binding of DC-HIL to dermatophytic fungi induces tyrosine phosphorylation and potentiates antigen presenting cell function. *Journal of Immunology*, *183*, 5190–5198.

Dahlgren, K. N., Manelli, A. M., Stine, W. B., Jr., Baker, L. K., Krafft, G. A., & LaDu, M. J. (2002). Oligomeric and fibrillar species of amyloid-beta peptides differentially affect neuronal viability. *The Journal of Biological Chemistry, 277*, 32046–32053.

Diaz-Ortiz, M. E., Seo, Y., Posavi, M., Cordon, M. C., Clark, E., Jain, N., Charan, R., Gallagher, M. D., Unger, T. L., Amari, N., Skrinak, R. T., Davila-Rivera, R., Brody, E. M., Han, N., Zack, R., Van Deerlin, V. M., Tropea, T. F., Luk, K. C., Lee, E. B., ... Chen-Plotkin, A. S. (2022). GPNMB confers risk for Parkinson's disease through interaction with α-synuclein. *Science, 377*, eabk0637.

Doroszkiewicz, J., Kulczńska-Przybik, A., Dulewicz, M., Borawska, R., Zajkowska, M., Slowik, A., & Mroczko, B. (2023). Potential utility of cerebrospinal fluid glycoprotein nonmetastatic melanoma protein B as a neuroinflammatory diagnostic biomarker in mild cognitive impairment and Alzheimer's disease. *Journal of Clinical Medicine, 12*, 4689.

Frenkel, D., Wilkinson, K., Zhao, L., Hickman, S. E., Means, T. K., Puckett, L., Farfara, D., Kingery, N. D., Weiner, H. L., & El Khoury, J. (2013). Scara1 deficiency impairs clearance of soluble amyloid-β by mononuclear phagocytes and accelerates Alzheimer's-like disease progression. *Nature Communications, 4*, 2030.

Friedman, B. A., Srinivasan, K., Ayalon, G., Meilandt, W. J., Lin, H., Huntley, M. A., Cao, Y., Lee, S. H., Haddick, P. C. G., Ngu, H., Modrusan, Z., Larson, J. L., Kaminker, J. S., van der Brug, M. P., & Hansen, D. V. (2018). Diverse brain myeloid expression profiles reveal distinct microglial activation states and aspects of Alzheimer's disease not evident in mouse models. *Cell Reports, 22*, 832–847.

Goldstein, J. L., Basu, S. K., & Brown, M. S. (1983). Receptor-mediated endocytosis of low-density lipoprotein in cultured cells. *Methods in Enzymology, 98*, 241–260.

Guerreiro, R., Wojtas, A., Bras, J., Carrasquillo, M., Rogaeva, E., Majounie, E., Cruchaga, C., Sassi, C., Kauwe, J. S. K., Younkin, S., Hazrati, L., Collinge, J., Pocock, J., Lashley, T., Williams, J., Lambert, J. C., Amouyel, P., Goate, A., Rademakers, R., ... Alzheimer Genetic Analysis Group. (2013). TREM2 variants in Alzheimer's disease. *The New England Journal of Medicine, 368*, 117–127.

Haass, C., & Selkoe, D. J. (2007). Soluble protein oligomers in neurodegeneration: Lessons from the Alzheimer's amyloid beta-peptide. *Nature Reviews. Molecular Cell Biology, 8*, 101–112.

Hakamata, H., Miyazaki, A., Sakai, M., Sakamoto, Y., Matsuda, H., Kihara, K., & Horiuchi, S. (1995). Differential effects of an acyl-coenzyme a:Cholesterol acyltransferase inhibitor on HDL-induced cholesterol efflux from rat macrophage foam cells. *FEBS Letters, 363*, 29–32.

Hales, C. M., Dammer, E. B., Deng, Q., Duong, D. M., Gearing, M., Troncoso, J. C., Thambisetty, M., Lah, J. J., Shulman, J. M., Levey, A. I., & Seyfried, N. T. (2016). Changes in the detergent-insoluble brain proteome linked to amyloid and tau in Alzheimer's disease progression. *Proteomics, 16*, 3042–3053.

Hanisch, U. K. (2013). Functional diversity of microglia—How heterogeneous are they to begin with? *Frontiers in Cellular Neuroscience, 7*, 65.

He, B., Shi, Y., Liang, Y., Yang, A., Fan, Z., Yuan, L., Zou, X., Chang, X., Zhang, H., Wang, X., Dai, W., Wang, Y., & Zhang, Q. (2018). Single-walled carbon-nanohorns improve biocompatibility over nanotubes by triggering less protein-initiated pyroptosis and apoptosis in macrophages. *Nature Communications, 9*, 2393.

Hee, J. S., Mitchell, S. M., Liu, X. R., & Leonhardt, R. M. (2017). Melanosomal formation of PMEL core amyloid is driven by aromatic residues. *Scientific Reports, 7*, 44064.

Hüttenrauch, M., Ogorek, I., Klafki, H., Otto, M., Stadelmann, C., Weggen, S., Wiltfang, J., & Wirths, O. (2018). Glycoprotein NMB: A novel Alzheimer's disease associated marker expressed in a subset of activated microglia. *Acta Neuropathologica Communications, 6*, 108.

Jumper, J., Evans, R., Pritzel, A., Green, T., Figurnov, M., Ronneberger, O., Tunyasuvunakool, K., Bates, R., Žídek, A., Potapenko, A., Bridgland, A., Meyer, C., Kohl, S. A. A., Ballard, A. J., Cowie, A., Romera-Paredes, B., Nikolov, S., Jain, R., Adler, J., ... Hassabis, D. (2021). Highly accurate protein structure prediction with AlphaFold. *Nature, 596*, 583–589.

Kamphuis, W., Kooijman, L., Schetters, S., Orre, M., & Hol, E. M. (2016). Transcriptional profiling of CD11c-positive microglia accumulating around amyloid plaques in a mouse model for Alzheimer's disease. *Biochimica et Biophysica Acta, 1862*, 1847–1860.

Kanzawa, T., Sawada, M., Kato, K., Yamamoto, K., Mori, H., & Tanaka, R. (2000). Differentiated regulation of allo-antigen presentation by different types of murine microglial cell lines. *Journal of Neuroscience Research, 62*, 383–388.

Kawahara, K., Gotoh, T., Oyadomari, S., Kajizono, M., Kuniyasu, A., Ohsawa, K., Imai, Y., Kohsaka, S., Nakayama, H., & Mori, M. (2001). Co-induction of argininosuccinate synthetase, cationic amino acid transporter-2, and nitric oxide synthase in activated murine microglial cells. *Brain Research. Molecular Brain Research, 90*, 165–173.

Kawahara, K., Hirata, H., Ohbuchi, K., Nishi, K., Maeda, A., Kuniyasu, A., Yamada, D., Maeda, T., Tsuji, A., Sawada, M., & Nakayama, H. (2016). The novel monoclonal antibody 9F5 reveals expression of a fragment of GPNMB/osteoactivin processed by furin-like protease(s) in a subpopulation of microglia in neonatal rat brain. *Glia, 64*, 1938–1961.

Kawahara, K., Suenobu, M., Ohtsuka, H., Kuniyasu, A., Sugimoto, Y., Nakagomi, M., Fukasawa, H., Shudo, K., & Nakayama, H. (2014). Cooperative therapeutic action of retinoic acid receptor and retinoid X receptor agonists in a mouse model of Alzheimer's disease. *Journal of Alzheimer's Disease, 42*, 587–605.

Kawahara, K., Yoshida, A., Koga, K., Yokoo, S., Kuniyasu, A., Gotoh, T., Sawada, M., & Nakayama, H. (2009). Marked induction of inducible nitric oxide synthase and tumor necrosis factor-α in rat CD40+ microglia by comparison to CD40− microglia. *Journal of Neuroimmunology, 208*, 70–79.

Kim, T., Vidal, G. S., Djurisic, M., William, C. M., Birnbaum, M. E., Garcia, K. C., Hyman, B. T., & Shatz, C. J. (2013). Human LilrB2 is a β-amyloid receptor and its murine homolog PirB regulates synaptic plasticity in an Alzheimer's model. *Science, 341*, 1399–1404.

Krasemann, S., Madore, C., Cialic, R., Baufeld, C., Calcagno, N., Fatimy, R. E. I., Beckers, L., O'Loughlin, E., Xu, Y., Fanek, Z., Greco, D. J., Smith, S. T., Tweet, G., Humulock, Z., Zrzavy, T., Conde-Sanroman, P., Gacias, M., Weng, Z., Chen, H., ... Butovsky, O. (2017). The TREM2-APOE pathway drives the transcriptional phenotype of dysfunctional microglia in neurodegenerative diseases. *Immunity, 47*, 566–581. e9.

Laurén, J., Gimbel, D. A., Nygaard, H. B., Gilbert, J. W., & Strittmatter, S. M. (2009). Cellular prion protein mediates impairment of synaptic plasticity by amyloid-beta oligomers. *Nature, 457*, 1128–1132.

Lee, S. H., Meilandt, W. J., Xie, L., Gandham, V. D., Ngu, H., Barck, K. H., Rezzonico, M. G., Imperio, J., Lalehzadeh, G., Huntley, M. A., Stark, K. L., Foreman, O., Carano, R. A. D., Friedman, B. A., Sheng, M., Easton, A., Bohlen, C. J., & Hansen, D. V. (2021). Trem2 restrains the enhancement of tau accumulation and neurodegeneration by β-amyloid pathology. *Neuron, 109*, 1283–1301. e6.

Mirdita, M., Schütze, K., Moriwaki, Y., Heo, L., Ovchinnikov, S., & Steinegger, M. (2022). ColabFold: Making protein folding accessible to all. *Nature Methods, 19*, 679–682.

Miyanishi, M., Tada, K., Koike, M., Uchiyama, Y., Kitamura, T., & Nagata, S. (2007). Identification of Tim4 as a phosphatidylserine receptor. *Nature, 450*, 435–439.

Moloney, E. B., Moskites, A., Ferrari, E. J., Isacson, O., & Hallett, P. J. (2018). The glycoprotein GPNMB is selectively elevated in the

substantia nigra of Parkinson's disease patients and increases after lysosomal stress. *Neurobiology of Disease*, *120*, 1–11.

Nakanishi, H. (2020). Microglial cathepsin B as a key driver of inflammatory brain disease and brain aging. *Neural Regeneration Research*, *15*, 25–29.

Oakley, H., Cole, S. L., Logan, S., Maus, E., Shao, P., Craft, J., Guillozet-Bongaarts, A., Ohno, M., Disterhoft, J., Van Eldik, L., Berry, R., & Vassar, R. (2006). Intraneuronal beta-amyloid aggregates, neurodegeneration, and neuron loss in transgenic mice with five familial Alzheimer's disease mutations: Potential factors in amyloid plaque formation. *The Journal of Neuroscience*, *26*, 10129–10140.

Ohsawa, K., Imai, Y., Nakajima, K., & Kohsaka, S. (1997). Generation and characterization of a microglial cell line, MG5, derived from a p53-deficient mouse. *Glia*, *21*, 285–298.

Prinz, M., Masuda, T., Wheeler, M. A., & Quintana, F. J. (2021). Microglia and central nervous system-associated macrophages-from origin to disease modulation. *Annual Review of Immunology*, *39*, 251–277.

Qin, W., Wang, H., Zhong, W., Bai, J., Qiao, J., & Lin, Z. (2021). Amyloidosis cutis dyschromica cases caused by GPNMB mutations with different inheritance patterns. *Journal of Dermatological Science*, *104*, 48–54.

Sadleir, K. R., Eimer, W. A., Cole, S. L., & Vassar, R. (2015). Aβ reduction in BACE1 heterozygous null 5XFAD mice is associated with transgenic APP level. *Molecular Neurodegeneration*, *10*, 1.

Satoh, J., Kino, Y., Yanaizu, M., Ishida, T., & Saito, Y. (2019). Microglia express GPNMB in the brains of Alzheimer's disease and Nasu-Hakola disease. *Intractable and Rare Diseases Research*, *8*, 120–128.

Sawada, M., Suzumura, A., Yamamoto, H., & Marunouchi, T. (1990). Activation and proliferation of the isolated microglia by colony stimulating factor-1 and possible involvement of protein kinase C. *Brain Research*, *509*, 119–124.

Shibuya, Y., Chang, C. C. Y., Huang, L.-H., Bryleva, E., & Chang, T.-Y. (2014). Inhibiting ACAT1/SOAT1 in microglia stimulates autophagy-mediated lysosomal proteolysis and increases Aβ1-42 clearance. *The Journal of Neuroscience*, *34*, 14484–14501.

Shikano, S., Bonkobara, M., Zukas, P. K., & Ariizumi, K. (2001). Molecular cloning of a dendritic cell-associated transmembrane protein, DC-HIL, that promotes RGD-dependent adhesion of endothelial cells through recognition of heparin sulfate proteoglycans. *The Journal of Biological Chemistry*, *276*, 8125–8134.

Shimizu, E., Kawahara, K., Kajizono, M., Sawada, M., & Nakayama, H. (2008). IL-4-induced selective clearance of oligomeric β-amyloid peptide$_{1-42}$ by rat primary type 2 microglia. *Journal of Immunology*, *181*, 6503–6513.

Smith, A. M., Davey, K., Tsartsalis, S., Khozoie, C., Fancy, N., Tang, S. S., Liaptsi, E., Weinert, M., McGarry, A., Muirhead, R. C. J., Gentleman, S., Owen, D. R., & Matthews, P. M. (2022). Diverse human astrocyte and microglial transcriptional responses to Alzheimer's pathology. *Acta Neuropathologica*, *143*, 75–91.

Söderberg, O., Gullberg, M., Jarvius, M., Ridderstråle, K., Leuchowius, K. J., Jarvius, J., Wester, K., Hydbring, P., Bahram, F., Larsson, L. G., & Landegren, U. (2006). Direct observation of individual endogenous protein complexes *in situ* by proximity ligation. *Nature Methods*, *3*, 995–1000.

Song, W. M., Joshita, S., Zhou, Y., Ulland, T. K., Gilfillan, S., & Colonna, M. (2018). Humanized TREM2 mice reveal microglia-intrinsic and -extrinsic effects of R47H polymorphism. *The Journal of Experimental Medicine*, *215*, 745–760.

Sturchler-Pierrat, C., Abramowski, D., Duke, M., Wiederhold, K. H., Mistl, C., Rothacher, S., Ledermann, B., Bürki, K., Frey, P., Paganetti, P. A.,

Waridel, C., Calhoun, M. E., Jucker, M., Probst, A., Staufenbiel, M., & Sommer, B. (1997). Two amyloid precursor protein transgenic mouse models with Alzheimer disease-like pathology. *Proceedings of the National Academy of Sciences of the United States of America*, *94*, 13287–13292.

Suzumura, A., Mezitis, S. G., Gonatas, N. K., & Silberberg, D. H. (1987). MHC antigen expression on bulk isolated macrophage-microglia from newborn mouse brain: Induction of Ia antigen expression by gamma-interferon. *Journal of Neuroimmunology*, *15*, 263–278.

Theos, A. C., Truschel, S. T., Raposo, G., & Marks, M. S. (2005). The Silver locus product Pmel17/gp100/Silv/ME20: Controversial in name and in function. *Pigment Cell Research*, *18*, 322–336.

van Dyck, C. H., Swanson, C. J., Aisen, P., Bateman, R. J., Chen, C., Gee, M., Kanekiyo, M., Li, D., Reyderman, L., Cohen, S., Froelich, L., Katayama, S., Sabbagh, M., Veilas, B., Watson, D., Dhadda, S., Irizarry, M., Kramer, L. D., & Iwatsubo, T. (2023). Lecanemab in early Alzheimer's disease. *The New England Journal of Medicine*, *388*, 9–21.

Walsh, D. M., Lomakin, A., Benedek, G. B., Condron, M. M., & Teplow, D. B. (1997). Amyloid beta-protein fibrillogenesis: Detection of a protofibrillar intermediate. *The Journal of Biological Chemistry*, *272*, 22364–22372.

Yang, C. F., Lin, S. P., Chiang, C. P., Wu, Y. H., H'ng, W. S., Chang, C. P., Chen, Y. T., & Wu, J. Y. (2018). Loss of GPNMB causes autosomal-recessive amyloidosis cutis dyschromica in humans. *American Journal of Human Genetics*, *102*, 219–232.

Yu, Y., & Ye, R. D. (2015). Microglial Aβ receptors in Alzheimer's disease. *Cellular and Molecular Neurobiology*, *35*, 71–83.

Zhao, Y., Wu, X., Li, X., Jiang, L. L., Gui, X., Liu, Y., Sun, Y., Zhu, B., Piña-Crespo, J. C., Zhang, M., Zhang, N., Chen, X., Bu, G., An, Z., Huang, T. Y., & Xu, H. (2018). TREM2 is a receptor for β-amyloid that mediates microglial function. *Neuron*, *97*, 1023–1031. e7.

Zhu, Z., Liu, Y., Li, X., Zhang, L., Liu, H., Cui, Y., Wang, Y., & Zhao, D. (2022). GPNMB mitigates Alzheimer's disease and enhances autophagy via suppressing the mTOR signal. *Neuroscience Letters*, *767*, 136300.

Zucca, F. A., Vanna, R., Cupaioli, F. A., Bellei, C., Palma, A. D., Silvestre, D. D., Mauri, P., Grassi, S., Prinetti, A., Casella, L., Sulzer, D., & Zecca, L. (2018). Neuromelanin organelles are specialized autolysosomes that accumulate undegraded proteins and lipids in aging human brain and are likely involved in Parkinson's disease. *NPJ Parkinsons Disease*, *4*, 17.

SUPPORTING INFORMATION

Additional supporting information can be found online in the Supporting Information section at the end of this article.